Title

E-cigarettes compromise the gut barrier and trigger inflammation

Journal

iScience, 24(2)

ISSN

2589-0042

Authors

Sharma, Aditi

Lee, Jasper

Fonseca, Ayden G

et al.

Publication Date

2021-02-01

DOI

10.1016/j.isci.2021.102035

Peer reviewed

iScience

CellPress
OPEN ACCESS

Article

E-cigarettes compromise the gut barrier and trigger inflammation

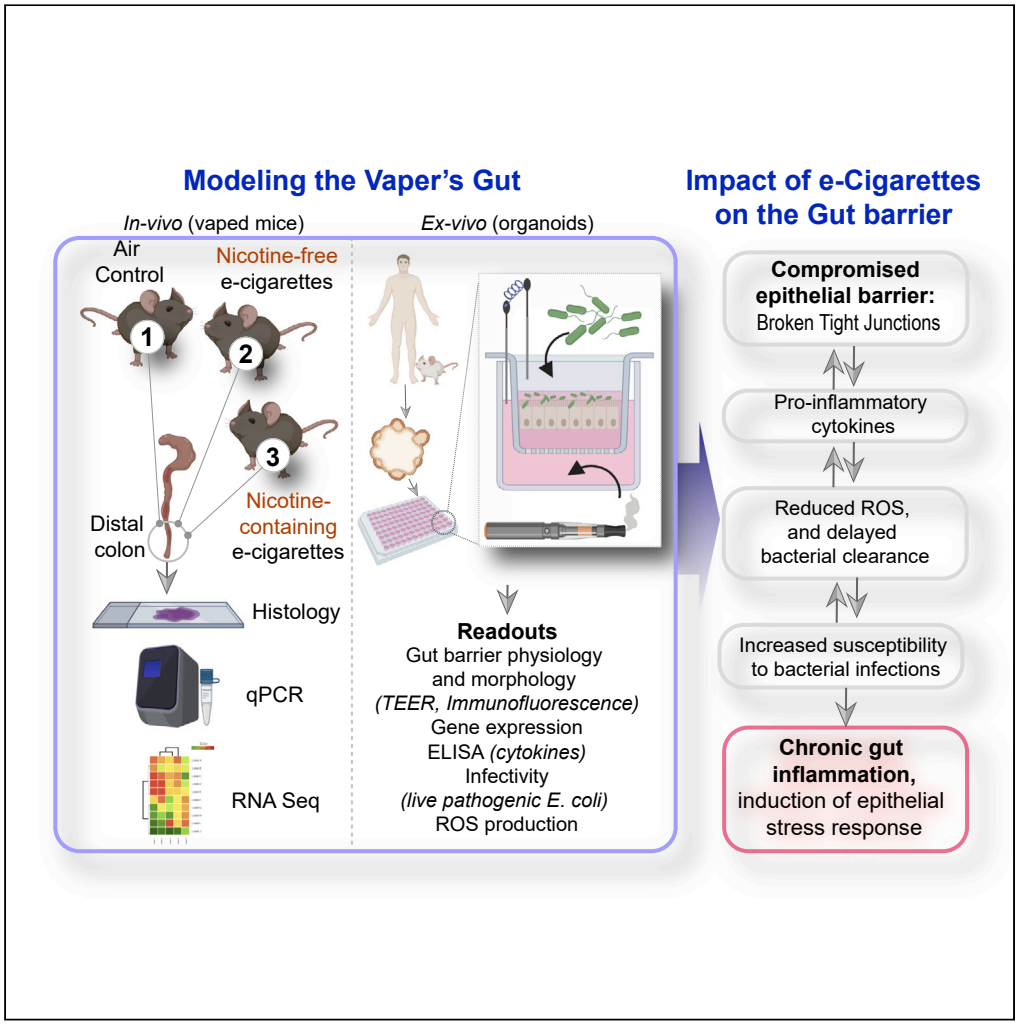

Aditi Sharma, Jasper Lee, Ayden G. Fonseca, ..., Laura E. Crotty-Alexander, Pradipta Ghosh, Soumita Das

lca@ucsd.edu (L.E.C.-A.)
prghosh@health.ucsd.edu (P.G.)
sodas@health.ucsd.edu (S.D.)

HIGHLIGHTS

Chronic vaping disrupts the gut barrier and triggers inflammation

Transcriptome studies reveal the broad impact of e-cig on gut health

Enteroid monolayers reveal that e-liquid, not nicotine, is the culprit

Chronic exposure to e-cig increases susceptibility to bacterial infection

Sharma et al., iScience 24, 102035
February 19, 2021
https://doi.org/10.1016/j.isci.2021.102035

iScience

CellPress
OPEN ACCESS

Article

E-cigarettes compromise the gut barrier and trigger inflammation

Aditi Sharma,[1,9] Jasper Lee,[1,9] Ayden G. Fonseca,[2,9] Alex Moshensky,[3] Taha Kothari,[1] Ibrahim M. Sayed,[1,8] Stella-Rita Ibeawuchi,[1] Rama F. Pranadinata,[2] Jason Ear,[2,3] Debashis Sahoo,[4,5,6] Laura E. Crotty-Alexander,[3,7,*] Pradipta Ghosh,[2,3,6,7,10,*] and Soumita Das[1,6,*]

SUMMARY

E-cigarette usage continues to rise, yet the safety of e-cigarette aerosols is questioned. Using murine models of acute and chronic e-cigarette aerosol inhalation, murine colon transcriptomics, and murine and human gut-derived organoids in co-culture models, we assessed the effects of e-cigarette use on the gut barrier. Histologic and transcriptome analyses revealed that chronic, but not acute, nicotine-free e-cigarette use increased inflammation and reduced expression of tight junction (TJ) markers. Exposure of murine and human enteroid-derived monolayers (EDMs) to nicotine-free e-cigarette aerosols alone or in co-culture with bacteria also causes barrier disruption, downregulation of TJ protein, and enhanced inflammation in response to infection. These data highlight the harmful effects of "non-nicotine" component of e-cigarettes on the gut barrier. Considering the importance of an intact gut barrier for host fitness and the impact of gut mucosal inflammation on a multitude of chronic diseases, these findings are broadly relevant to both medicine and public health.

INTRODUCTION

Electronic nicotine delivery systems, commonly referred to as e-cigarettes and vaping devices, were introduced to the international market in 2007 (Etter and Bullen, 2011). Since then, e-cigarettes have become widely popular in the United States (CDC; and United-States, 2016), primarily among the nation's youth. A large amount of research surrounding its regulation and consumption has been focused on the addictive nicotine component in these devices; however, recent studies have increasingly begun to scrutinize the harmful potential of the chemicals in the e-liquids, e.g., propylene glycol (PG), glycerol (VG), flavorings, and contaminants (Alasmari et al., 2017, 2019; Bozier et al., 2020; Khlystov and Samburova, 2016; Perez and Crotty Alexander, 2020; Yu et al., 2016). The PG:VG ratio is a key determinant of the amount of vapor that is optimal for maintaining the flavor, whereas the composition of the e-liquid determines the exact proportions of the ~50–150 chemicals that are generated via heat-mediated pyrolysis and chemical decomposition (Margham et al., 2016). Despite the presence of these wide ranges of multiple chemicals, few regulations control the chemical composition of e-cigarettes, and they remain popular as a risk-free alternative to combustible cigarettes.

This concept of risk-free use has recently been challenged. For example, morbidity and mortality among teenagers and young adults owing to e-cigarette or vaping product use-associated lung injury (King et al., 2020) created a public health crisis in 2019–2020; a single (non-nicotine) chemical in the e-liquids, i.e., vitamin E acetate was found to be the culprit (Blount et al., 2020). *In vitro* and *ex vivo* studies have already shown that e-liquids induce inflammatory responses and alter innate immune defenses in myeloid and primary airway epithelial cells (Muthumalage et al., 2017; Scott et al., 2018; Wu et al., 2014). Mice exposed to e-cigarette aerosols for 2 weeks were found to have impaired pulmonary bacterial and viral clearance (Hwang et al., 2016; Sussan et al., 2015), which suggested increased susceptibility to influenza and coronavirus infections in particular. Evidence of pulmonary and systemic inflammation has also been found in the serum (Singh et al., 2019) and bronchoalveolar lavage (Song et al., 2020) samples from human e-cigarette-users, with elevated biomarkers of inflammation, e.g., interleukin (IL)-1β, IL-6, IL-8, IL-13, and interferon (IFN)-γ. Furthermore, mechanisms that link the use of e-cigarettes to an increased risk of cancers (Tang et al., 2019) or of cancer progression (Mravec et al., 2020) have been proposed, and e-cigarettes have

[1]Department of Pathology, University of California, San Diego, CA 92093, USA

[2]Department of Cellular and Molecular Medicine, University of California, San Diego, CA 92093, USA

[3]Department of Medicine, University of California, San Diego, CA 92093, USA

[4]Department of Pediatrics, University of California, San Diego, CA 92093, USA

[5]Department of Computer Science and Engineering, Jacobs School of Engineering, University of California, San Diego, CA 92093, USA

[6]Rebecca and John Moore Comprehensive Cancer Center, University of California, San Diego, CA 92093, USA

[7]Veterans Affairs Medical Center, VA San Diego Healthcare System, La Jolla, San Diego, CA 92093, USA

[8]Additional Affiliation: Department of Medical Microbiology and Immunology, Faculty of Medicine, Assiut University, Assiut, Egypt

[9]These authors contributed equally

[10]Lead contact

*Correspondence: lca@ucsd.edu (L.E.C.-A.), prghosh@health.ucsd.edu (P.G.), sodas@health.ucsd.edu (S.D.)

https://doi.org/10.1016/j.isci.2021.102035

been shown to induce DNA damage (independent of nicotine [Yu et al., 2016]) while reducing repair pathways (Lee et al., 2018). In light of these studies, an NIH-funded panel declared that all chemical components of e-cigarette and vaping aerosols have the potential to adversely affect health (Crotty Alexander et al., 2020), both in the heart and lungs and throughout the body (Crotty Alexander et al., 2020).

Here we set out to assess the impact of e-cigarette aerosol inhalation (with or without nicotine) on the gastrointestinal tract. The gut is resident to diverse microbiota, and its handling of and response to the same is known to regulate several chronic diseases such as inflammatory bowel diseases (IBDs), obesity, cardiovascular diseases, cancers, and rheumatoid arthritis (Gilbert et al., 2016). Studies on human subjects have shown that e-cigarette use significantly modulates the oral microbiome (Pushalkar et al., 2020) but not the gut microbiome (Stewart et al., 2018). Studies in mice, however, have shown that e-cigarettes alter epithelial mucus profiles and microbial diversity (Allais et al., 2016) and that such changes may induce inflammation and decrease the integrity of the gut barrier (Fricker et al., 2018). Although e-cigarette use is long suspected to negatively impact human gastrointestinal physiology, based on the numerous digestive symptoms reported by vapers (Hua et al., 2013), little to nothing is known as to how e-cigarette use may impact the human gut barrier. Using a combination of mouse models, transcriptomics, and murine and human gut-derived organoids as *ex vivo* near-physiologic model systems, here we expose the hitherto unknown effects of e-cigarettes on the gastrointestinal tract and provide insights into the potential long-term effects of e-cigarettes on health.

RESULTS

Daily e-cigarette aerosol inhalation drives inflammation in the colon and reduces the expression of genes related to barrier function

To establish the *in vivo* effect of inhalation of these aerosols on the colon, the distal colon was harvested from mice exposed daily to e-cigarette aerosols (1 h/day) at two time points: 1 week (resembling acute exposure) and 3 months (resembling chronic exposure) (Figure 1A). Because the most common chemicals in e-cigarette aerosols are nicotine and humectants (propylene glycol and vegetable glycerin), we utilized nicotine-free and nicotine-containing (6 mg/mL) e-liquids with a 70:30 ratio of propylene glycol and vegetable glycerol (PG:VG) within a KangerSubtank attached to a box Mod e-device and used exposure chambers with room air for controls (Figure 1A). This low concentration of nicotine (6 mg/mL) was selected on the basis of several published works (ranging typically between ~6 and 9 mg/mL) and the amount present in the most popular brands (Cox et al., 2016; Dawkins et al., 2016; Stewart et al., 2018). The ratio of 70:30 PG:VG was chosen because it is the most commonly used and preferred *ratio as per consumer experience* (Smith et al., 2020). H&E staining of distal colons from mice acutely exposed to nicotine-free (vehicle only) e-cigarette aerosols (e-cig) for 1 week demonstrated small, infrequent patches of leukocyte infiltration in the submucosal layers (Figure 1B, *left; asterisk*). Acute exposure to nicotine-containing aerosols (e-cig + nicotine) was associated with infrequent patches of epithelial erosions. By contrast, chronic e-cig exposure over 3 months led to large submucosal inflammatory infiltrates within the colon (Figure 1B, *right*). No inflammatory infiltrates were seen in air controls, and only smaller and infrequent infiltrates were present in colons of mice chronically exposed to nicotine-containing e-cig (e-cig + nicotine).

Markers of gut epithelial tight junctions (TJs), e.g., occludin (OCLN), zonula occludens (ZO)-1 (TJP1), and Claudin-2 (CLDN2) had significantly reduced gene expression in mice chronically exposed to nicotine-free aerosols (e-cig) compared with air controls (Figure 1C). The fact that e-cig exposure affects the levels of Claudin-2, a major regulator of TJ-specific obliteration of the intercellular space (Kubota et al., 1999), but not its counterpart Claudin-1 (Figure 1C), which is specialized for TJ integrity in the skin epidermis, indicates that the effects of e-cig on TJs may be gut specific. No reduction was observed in any of the barrier function genes in mice exposed to nicotine-containing e-cigarettes. No significant differences were observed in the levels of pro-inflammatory cytokines MCP1 or IL-8 in the chronically exposed mice (Figure S1). Finally, no statistically significant differences were observed in the transcript levels of TJ markers and pro-inflammatory cytokines in acute exposures between any conditions (Figure S1).

These findings indicate that chronic, but not acute, exposure to aerosols of nicotine-free e-cigarettes is sufficient to trigger inflammation in the gut and that such inflammation is associated with reduced expression of markers of epithelial TJs. Findings also suggest that concomitant exposure to nicotine may ameliorate both phenotypes.

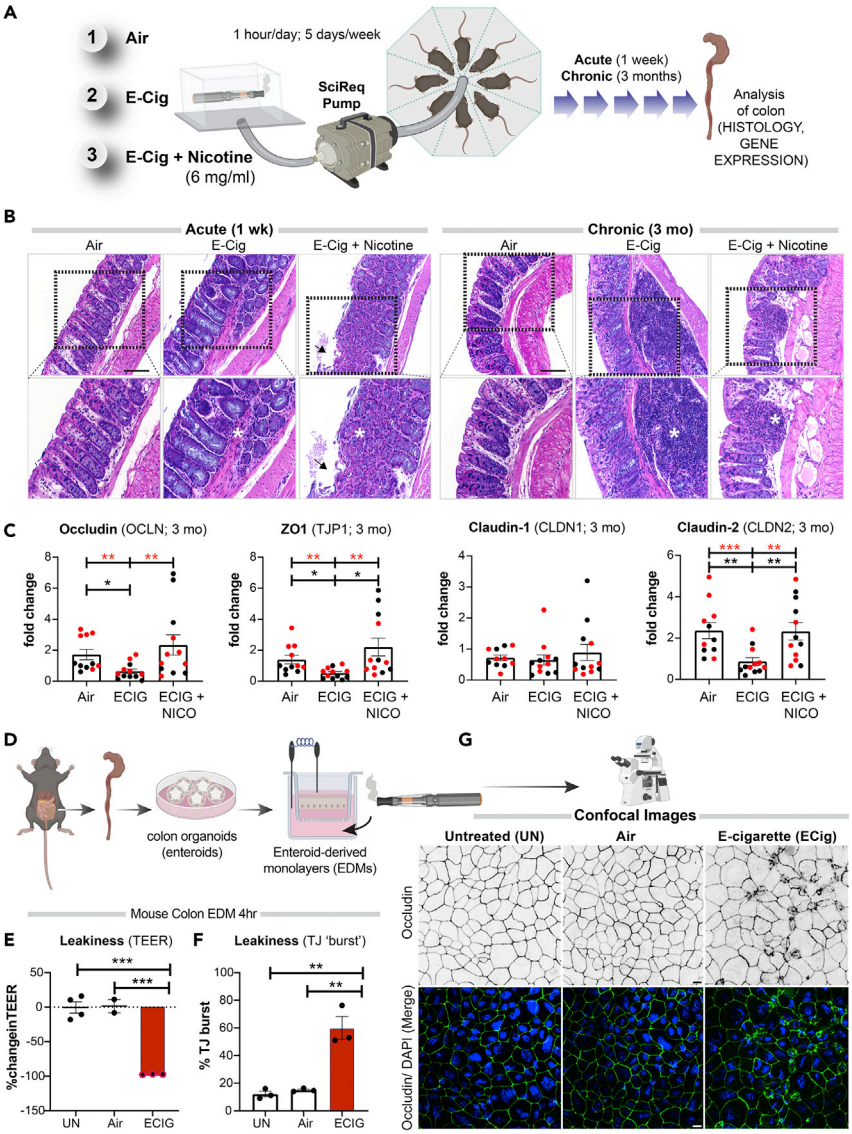

Figure 1. Electronic cigarettes trigger inflammation in the murine distal colon and disrupt the integrity of the murine gut barrier

(A) Schematic displays the key aspects of the murine model of vaping used in this study. Mice were exposed to air (negative control), nicotine-free e-cig (e-cig alone; MOD brand), or nicotine-containing e-cig (e-cig + 6 mg/mL nicotine) for 1 week or 3 months.

(B) Hematoxylin-eosin staining of distal colons after 1 week (left) or 3 months (right) of exposure to e-cig. Asterisks, inflammatory infiltrates; arrowheads, epithelial erosions.

(C) Bar graphs display the relative levels of expression of genes in the colon (black dots, male mice; red dots, female mice) that encode proteins that regulate epithelial tight junctions. Data are displayed as mean ± SEM. Statistical significance was estimated using either one-way ANOVA with Tukey's test (black *) or Mann-Whitney's test (red *); *p<0.05, **p <0.01 and ***p <0.001.

(D) Schematic displays the key aspects of *ex vivo* disease modeling to interrogate the impact of vaping on the murine colonic epithelial barrier.

(E) Bar graphs display the percent change in TEER. Data are displayed as mean ± SEM (n = 3–4 independent experiments). UN, normal media; Air, air-infused media.

(F and G) EDMs were treated as indicated, fixed and stained for occludin (green) and DAPI (blue, nuclei), and analyzed by confocal microscopy. Bar graphs in (F) display the percent increase in the tight junction (TJ) "bursts" (indicative of disrupted TJs). Data are displayed as mean ± SEM (n = 3 fields/condition; 40–50 tricellular TJs/field). Statistical significance was estimated using one-way ANOVA with Tukey's test; **p <0.01. Confocal microscopic images in (G) are representative of EDMs, either untreated (UN) or after 4 h of treatment with air or e-cig-infused media. Scale bar, 10 μm.

E-cigarettes disrupt the integrity of the gut barrier

An intact gut barrier is an important first-line defense. To determine if the observed decrease in colon TJ markers in mice exposed to e-cigs is a direct consequence of circulating chemicals inhaled in the aerosols on the gut epithelial barrier, we used an *ex vivo* near-physiologic model system called the "gut-in-a-dish" (Figure 1D) (Ghosh et al., 2020). In this model, crypt-derived stem cells isolated from mouse colon (see the Transparent methods section) were used to generate organoids and later differentiated into polarized enteroid-derived monolayers (EDMs). The EDMs are also widely believed to be a model that is superior to cultured colon cancer cell lines (e.g., Caco2) because (1) they have been validated as model systems that closely resemble the physiologic gut lining in which all cell types (enterocytes, goblet, paneth enteroendocrine, and tuft cells) are proportionately represented (Foulke-Abel et al., 2014; Mahe et al., 2013; Miyoshi and Stappenbeck, 2013; Noel et al., 2017); (2) they are not transformed and yet allow culturing over several passages so that they can be used to ensure reproducibility of meaningful functional studies; and (3) because they preserve dimensionality, i.e., apicobasal polarity with functional tight junctions that can recreate the gut barrier *ex vivo*.

To dissect how e-cig-derived chemicals in the systemic circulation impact the gut barrier, we exposed the basolateral surfaces of the murine colonic EDMs to e-cigarette aerosol-infused media. As negative controls, we exposed the EDMs either to normal growth media ("UN") or to air-infused media ("Air"). We analyzed the integrity of the gut barrier using two readouts (Figure 1D): (1) paracellular permeability, as reflected by low trans-epithelial electrical resistance (TEER) and (2) molecular characterization of epithelial TJs by looking at the localization of occludin; this integral membrane protein allows us to not just visualize but also quantify the degree of TJ disruption. Exposure to nicotine-free e-cigarette aerosol media caused a significant drop in TEER (~% change value of $-97.3 \pm 0.3\%$) compared with untreated (UN, $-0.5 \pm 8.1\%$) and air-treated ($1.4 \pm 9.7\%$) controls (Figure 1E). Findings indicate a significant increase in paracellular permeability upon exposure to e-cig when compared with untreated ($p = 0.0002$) and air-treated ($p = 0.0004$) controls (Figure 1E). In e-cig-exposed EDMs, confocal microscopy showed a significantly increased "burst" tricellular TJs (these are specialized regions of the TJ where three or more cells come in contact [Furuse et al., 2014], and are also the regions where TJ disruption can be visualized/assessed first [Ghosh et al., 2020]) by $\sim 60.1 \pm 8.1\%$ when compared with untreated ($p = 0.0010$) and air-treated ($p = 0.0015$) controls (Figures 1F and 1G). These findings show that chemicals contained within the most basic e-cigarette aerosols have a direct disruptive effect on the epithelial barrier. Because the chemicals used to make the e-liquids and e-cig aerosols used in these studies (propylene glycol and glycerol) are found in >99% of all e-cigarettes, these data broadly apply to e-cigarettes and vaping devices.

Chronic exposure to inhaled e-cigarette aerosols induces stress responses in the colon

To determine the global impact of e-cigarettes on the gut, we next carried out RNA sequencing (RNA-seq) on the distal colons. Acute exposure to nicotine-free e-cigarettes did not significantly change gene expression in the colon (Figure S2A), whereas chronic exposure was associated with significant changes (Figure 2A). A differential expression analysis showed that chronic exposure to nicotine-free e-cigarettes was associated with a significant upregulation of 120 genes and downregulation of 75 genes (with a 30% false discovery rate, FDR) (Figure 2B; Table S1). Barring a handful of genes (arrowheads, Figures 2B and S2B), most of these differences were abolished when mice were exposed to nicotine-containing e-cigarettes (Figure 2B). TJ markers occludin and ZO1 were downregulated by nicotine-free, but not nicotine-containing, e-cigarettes (Figures 2C and 2D). Multiple pro-inflammatory cytokines were either elevated significantly (MCP1, IL-8, and TNF-α) or showed an increasing trend but did not reach significance (Cxcl2) (Figures 2E–2H). These RNA-seq findings are in agreement with our prior observations by histology (Figure 1B) and the targeted analyses of TJ markers by qPCR (Figure 1C), in that colons of mice exposed to nicotine-free, but not nicotine-containing, e-cig have impaired TJ markers and are inflamed.

Kyoto Encyclopedia of Genes and Genomes (KEGG) pathway (Figure 2I) and Gene Ontology (GO) (Figure S3) analyses revealed that the most enriched disease-related pathways were those that are involved in cellular sensing and response to external stress and stimuli (peroxisome proliferator-activated receptors [PPARs] and 5′ AMP-activated protein kinase [AMPK] signaling), cell death and programmed cell death, defense response to other organisms, metabolism (lipolysis, adipocytokine, and thermogenesis), and inflammation (cytokine and receptors). With regard to cytokine signaling, we noted that *il31ra* (subunit for IL6R), *il1r2* (decoy receptor for IL1R1), *ccl8* (a chemoattractant), *ear2* (chemoattractant), and *ilk* (activator of nuclear factor κB [NF-κB]) were upregulated, whereas *trim30a* (a suppressor of NF-κB) and *madcam1* (a

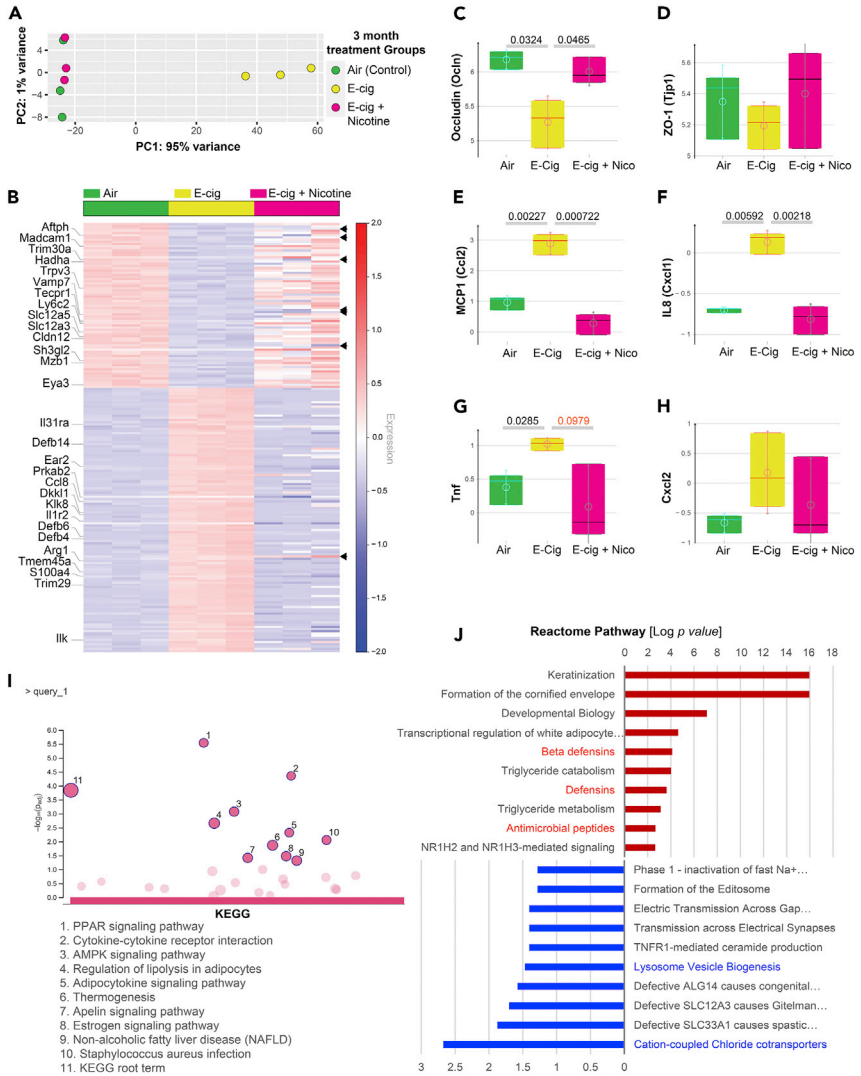

Figure 2. Nicotine-free, but not nicotine-containing, e-cigarettes trigger wide-ranging changes in gene expression in the colon

(A) Principal component analysis (PCA) of the topmost variable genes in the distal colons of the three groups of mice, all exposed to air or e-cig as indicated for 3 months. PCA identified air control and nicotine-containing e-cig group as similar to each other, but distinctly different from the e-cig alone group along the first principal component.

(B) Heatmap visualization of the differentially expressed genes between the three groups of mice. Each row represents one of the genes, whereas columns represent expression averages of replicates for each investigated group. Red color indicates relative over-expression, whereas blue color indicates relative under-expression. Top genes in the Reactome pathway analyses are marked on the left side. Arrowheads on the right side indicate a few genes that remained altered in both e-cig alone and e-cig + nicotine groups (see Figure S2B).

(C–H) Whisker plots display the levels of expression of the genes, as determined by RNA-seq encoding tight junction markers (occludin, C; ZO1, D; and pro-inflammatory cytokines (MCP1), E; IL-8, F; TNF-α, G; Cxcl2, H).

(I and J) KEGG (I) and Reactome (J) pathway analyses of the list of differentially expressed genes (see Table S1) reveal the most up or downregulated pathways. Red color indicates upregulation, whereas blue color indicates the downregulation of gene expression. No significant enrichment of pathways was seen in the list of downregulated genes by KEGG analyses.

cell-adhesion molecule required for leukocyte trafficking) were downregulated. No KEGG pathways were significantly enriched among the downregulated genes. A Reactome pathway (Figure 2J) analysis on the same gene sets showed enrichment of anti-microbial peptides, specifically beta-defensins (*Defb4, 6 and 14*), and de-enrichment of regulators of lysosome biogenesis (*sh3gl2, eya3, vamp7*) and chloride

transporters (*slc12a3, slc12a5*). Besides these statistically enriched pathways and processes, it is noteworthy that several cancer-related genes (*dkkl1, trim29, s100a4, tmem45a,* and *klk8*) were also upregulated (Figure 2B), and as expected, an enrichment of pathways for differentiation program in the colon (e.g., multiple Keratins; Figure 2J). Many of these differentiation-related genes continued to remain high despite nicotine (Figure S2B). These findings suggest the upregulation of two opposing programs in the colon that tightly regulate oncogenesis in the colon.

Chronic (repetitive) exposure to e-cigarettes disrupts the integrity of the human gut barrier and triggers inflammation

To translate the relevance of our findings in mice colon to the human gut, we generated organoids from colonic and ileal biopsies obtained from healthy human subjects (three independent donors, age range 29–71 years). These organoids were subsequently differentiated into EDMs and exposed either acutely (single exposure) or chronically (repeated exposures x3, each 4 h apart) prior to analyzing them at 24 h for barrier integrity and markers of inflammation using multiple modalities (see Figure 3A). An acute single exposure to e-cig was associated with a significant drop in TEER (−48.1 ± 5.5%) at 4 h (Figure 3B, *left*). However, much of that initial drop at 4 h was virtually reversed after 24 h to levels that were similar to untreated or air-treated control EDMs (UN = 41.7 ± 8.0%, Air = 49.1 ± 14.5% and e-cig = 23.6 ± 18.5% (Figure 3B, *right*). When the EDMs were subjected to 3x e-cig exposures, which is a more physiologic exposure based on human use patterns, the drop in TEER was sustained at 24 h (−59.96 ± 3.82%; Figure 3B, *right*).

We also confirmed that the observed drop in TEER in the colon-derived EDMs was also associated with a loss of structural integrity of the TJs. An acute single exposure was associated with only infrequent aberrant tricellular TJ morphology and a statistically insignificant "burst" appearance at 24 h (Figure 3C, *left*; Figure 3D, *arrowheads*). However, repeated 3x exposures resulted in a significant ∼3-fold increase in the percentage of burst TJs (Figure 3C, *right*; Figure 3E, *arrowheads*). The levels of transcripts of the membrane-integral TJ marker, occludin, increased after acute exposure (Figure 3F, *left*) but returned to normal levels at 24 h (Figure 3F, *right*; Figure S4). The levels of the peripheral TJ marker ZO1 was unchanged at 4 h after an acute exposure (Figure 3G, *left*), while there was a significant drop in gene expression of ZO1 after chronic repetitive multiple exposure (Figure 3G, *right*).

Because prior studies have implicated loss of epithelial barrier integrity as permissive to inflammation (Ghosh et al., 2020), we next investigated inflammatory gene expression in the e-cigarette-exposed EDMs by qPCR. Compared with untreated or air-treated controls, chronic repetitive exposure to e-cigarettes (but not single acute exposure) increased the expression of transcripts for all the pro-inflammatory cytokines tested (Figures 4A–4D). ELISA studies conducted on EDM supernatants confirmed that the protein levels of the pro-inflammatory cytokine IL-8 were significantly elevated (Figure 4E).

Similar findings were also observed in the case of human ileum-derived EDMs. TEER dropped significantly at 4 h after both single and 3x exposures (Figures S5A–S5C; ∼55% drop compared with control EDMs). The patterns of change in occludin and ZO1 were mirrored in the case of human ileum-derived EDMs (Figures S5D–S5G). A single acute exposure had little or no effect on cytokine transcripts (Figures S5H, S5J, S5L, and S5N), whereas chronic repetitive e-cigarette exposure caused increased IL-1B (Figure S5I), IL-6 (Figure S5K), IL-8 (Figure S5M), and MCP1 (Figure S5O).

Taken together, these physiologic (TEER), morphologic (burst appearance of TJs), and transcriptomic (qPCR assessment of markers of TJ transcripts) readouts are all in agreement, i.e., exposure to nicotine-free e-cigarette aerosols causes epithelial barrier dysfunction in the human gut. They also demonstrate that chronic (repetitive), but not acute (single), exposure is necessary for such disruption and that such disruption is associated with the induction of pro-inflammatory cytokines.

Chronic (repetitive) exposure of the gut epithelium to e-cigarette aerosols accentuates inflammatory responses to infections

Because the gut epithelial barrier of those who vape is concomitantly exposed to chemical components of e-cigarettes as well as luminal microbes, we exposed EDMs simultaneously to both stressors. First, we exposed the basolateral side of EDMs grown on Transwells to e-cigarette-infused media (mimicking the absorption of core chemicals contained within nicotine-free vaping aerosols into the blood stream and diffusion into tissues) and subsequently challenged the apical surface with live pathogenic microbes (to

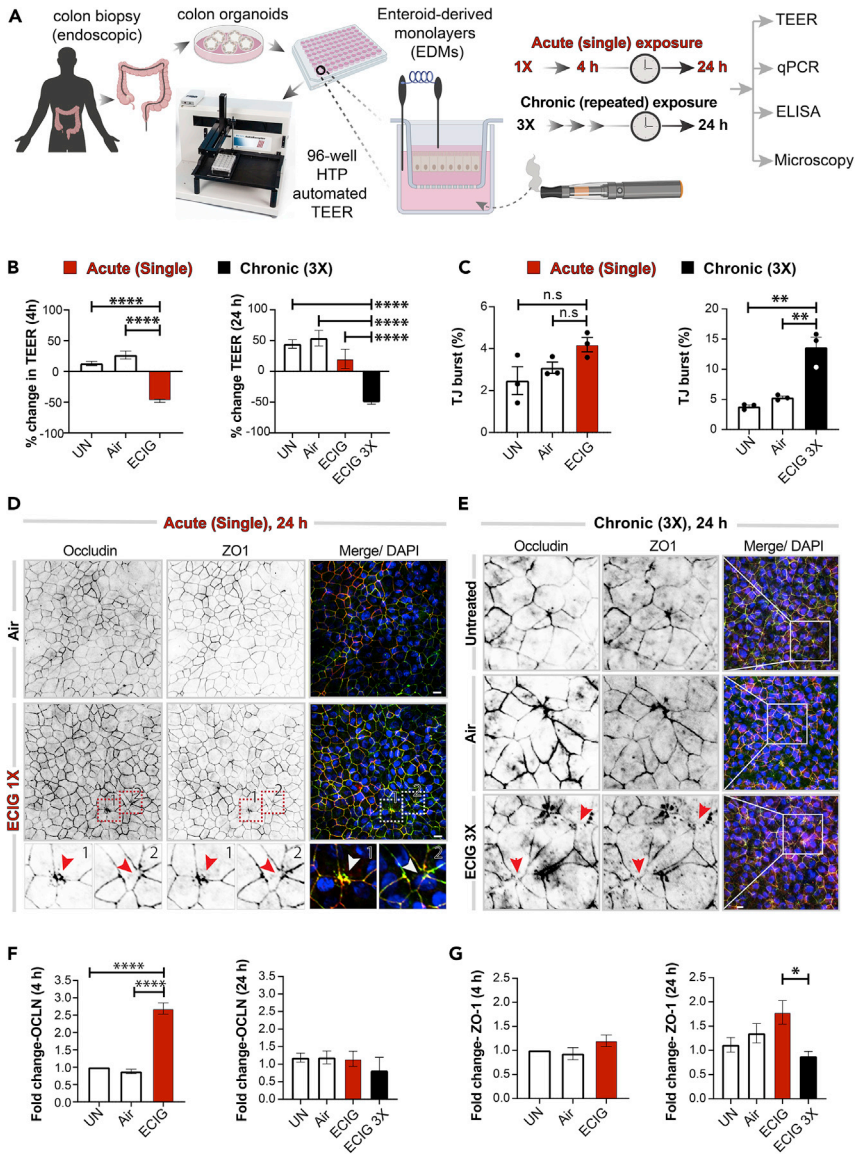

Figure 3. Chronic exposure to e-cigarettes disrupts the integrity of the human gut barrier, triggers inflammation

(A) Schematic displays the key aspects of *ex vivo* disease modeling to interrogate the impact of vaping on the human colonic epithelial barrier. Two modes of exposures (acute and chronic) were modeled and a variety of functional readouts were analyzed. UN, normal media; Air, air-infused media.

(B) Bar graphs display percent change in transepithelial electrical resistance (TEER) over time. Data are displayed as mean ± SEM (n = 3). Statistical significance was estimated using one-way ANOVA with Tukey's test; ****p <0.0001.

(C–E) EDMs were treated as indicated prior to fixation, and then stained for tight junction (TJ) marker occludin (green), ZO1 (red), and DAPI (blue, nuclei) and analyzed by confocal microscopy. Bar graphs in (C) display the percent increase in tight junction (TJ) "bursts." Data are displayed as mean ± SEM (n = 3 fields/condition). Statistical significance was estimated using one-way ANOVA with Tukey's test; **p <0.01; n.s., not significant. Confocal microscopic images representative of EDMs after 24 h of treatment with either a single (D) or repeated (3x; E) exposures to air (control) or nicotine-free e-cig vapor-infused media are shown. Scale bar, 10 μm. Insets "1" and "2" in (D) are displayed below as magnified panels and the arrowheads (red/white) in (D) and (E) point to examples of burst TJs.

(F and G) Bar graphs display the relative fold change in mRNA expression of tight junction markers (Occludin and ZO1) in human EDMs after acute (4 h) or chronic (24 h) exposure of e-cig vapor-infused media. Data are displayed as mean ± SEM (n = 3). Statistical significance was estimated using one-way ANOVA with Tukey's test; *p<0.05 and ****p <0.0001.

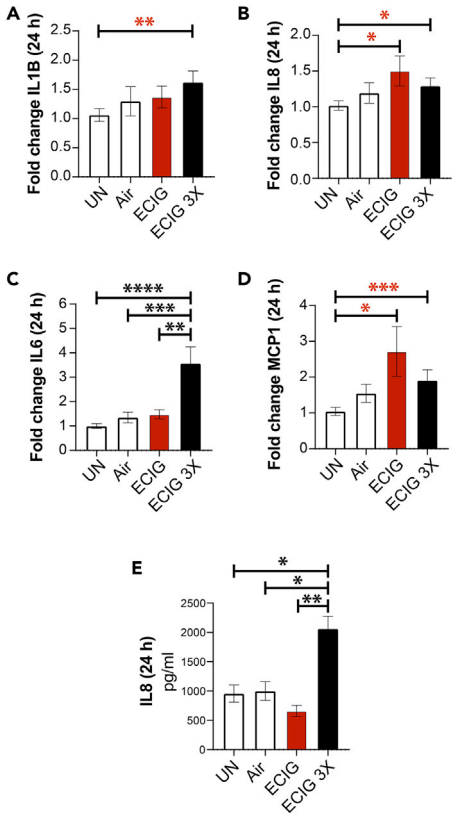

Figure 4. Chronic exposure to nicotine-free e-cigarette induces the expression of pro-inflammatory cytokines in the human colonic epithelium

(A–D) Bar graphs display the relative fold change in the levels of mRNA for pro-inflammatory cytokines. Data are shown as mean ± SEM (n = 3). UN, normal media; Air, air-infused media. Statistical significance was estimated using either one-way ANOVA with Tukey's test (black) or Mann-Whitney test (red); *p<0.05, **p <0.01, and ***p <0.001. (E) Bar graphs display the concentration of IL-8 released in the basolateral compartment of polarized EDMs after exposure to e-cig vapor-infused media. Data are shown as mean ± SEM (n = 3 independent experiments). Statistical significance was estimated using one-way ANOVA with Tukey's test; *p<0.05 and **p <0.01.

simulate luminal microbes) (Figure 5A). As before (in Figure 3), EDMs were either treated acutely (single exposure) or chronically (repeated exposures x3, each 4 h apart) with e-cig-infused media (ECIG X3). In the negative controls, which were exposed only to media (UN), the media were changed every 4 h (UNX3), just like the e-cig condition. We used the adherent invasive *E. coli (AIEC)-LF82*, a pathogen that was originally isolated from a patient with IBD (Boudeau et al., 1999). Compared with untreated controls, EDMs repeatedly exposed to e-cigarette aerosol media had a significant drop in the levels of occludin mRNA (Figure 5B, *left*) and significant increases in the levels of transcripts of inflammatory cytokines IL-1B, IL-8, and MCP1 (Figures 5C–5E). Levels of IL-6 also trended up but fell short of statistical significance (Figure 5F). ELISA studies confirmed that EDMs repeatedly exposed to e-cigarette aerosol media also secreted higher amounts of IL-8 (Figure 5G) and MCP1 (Figure 5H). Unlike the EDMs that were repeatedly exposed to e-cigarettes (3x), those exposed only once did not have a significant reduction in occludin (Figure 5B, *left*) or induction of proinflammatory cytokines (Figures 5C–5H). These findings indicate that exposure to the common core chemical components of e-cigarette aerosols is sufficient to make the gut hyperreactive to microbes and that repetitive exposure is necessary for such hyperresponsiveness.

Because cytokine production by epithelial cells after an infection is a culmination of multiple events during epithelial sensing and signaling that are triggered by microbes, we next asked how exposure to e-cigarettes impacts some of the early steps, i.e., infectivity of the gut epithelium and epithelial reaction to such infection by production of reactive oxygen species (ROS); the latter serves as a critical second messenger that modulates innate immune signaling in the gut epithelium (Jones et al., 2012). EDMs

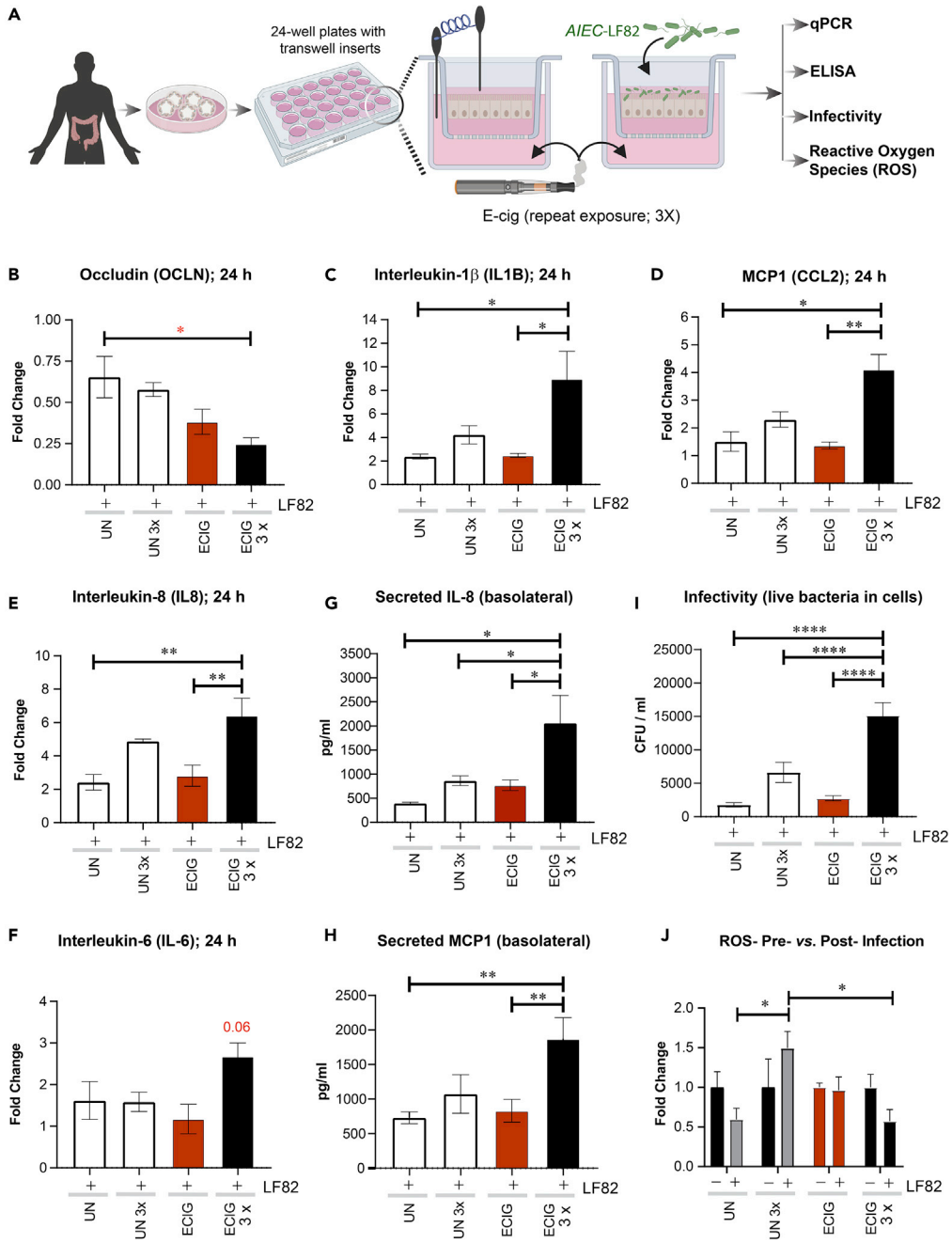

Figure 5. Chronic exposure to nicotine-free e-cigarette induces the expression of pro-inflammatory cytokines in the human colonic epithelium

(A) Schematic displays the overall experimental design for assessing how e-cig affects the gut epithelial response to infectious pathogenic microbes, e.g., *E. coli* strain AIEC-*LF-82*.

(B–F) Bar graphs display the relative fold change (compared to media control) in the levels of mRNA for pro-inflammatory cytokines. Data are shown as mean ± SEM (n = 3 independent experiments). Statistical significance was estimated using one-way ANOVA with Tukey's test; *p<0.05, **p <0.01.

(G and H) Bar graphs display the concentration of IL-8 (G) and MCP-1 (H) released in the basolateral compartment of polarized EDMs after exposure to e-cig vapor-infused media. Data are shown as mean ± SEM (n = 3 independent experiments). Statistical significance was estimated using one-way ANOVA with Tukey's test; *p<0.05 and **p <0.01.

(I) Bar graphs display the bacterial load internalized in EDMs pretreated as indicated with or without single or repeated exposure to e-cig vapor-infused media and then exposed to pathogenic *AIEC-LF82* for 3 h. Data are expressed as the

Figure 5. *Continued*
number of internalized bacteria to the infected control EDMs (untreated; i.e., not exposed to e-cig) and is represented as the mean ± SEM of three separate experiments. Statistical significance was estimated using one-way ANOVA with Tukey's test;**** p< 0.0001.
(J) Bar graphs display cellular accumulation of ROS, as determined by measuring the levels of oxidized DNA in the supernatant in the basolateral compartment of polarized EDMs after exposure to the indicated treatments. Data are represented as the mean ± SEM of three separate experiments. Statistical significance was estimated using one-way ANOVA with Tukey's test; *p<0.05.

exposed repeatedly to e-cig (3x) showed a statistically significant higher number of internalized bacteria compared with control EDMs after 3 h of infection, demonstrating decreased host defenses with higher infectivity of gut epithelium after e-cigarette exposure (Figure 5I). Finally, we found that repeated exposures of e-cigarette aerosol media (3x) followed by infection of EDMs were associated with a reduction in ROS (Figure 5J). Unlike the chronically exposed EDMs, those exposed only once did not show a significant increase in infectivity, nor did they show a significant reduction in ROS production (Figures 5I and 5J).

Taken together, these findings indicate that chronic repetitive exposure to e-cigarettes alters the gut epithelial cell response to infection with pathogenic microbes, characterized by higher infectivity and induction of pro-inflammatory cytokines and a failure to induce protective ROS. Because the overall composition of the gut microbes does not appear to be significantly altered among the subjects who consume e-cigarettes (Stewart et al., 2018), our findings show that e-cigarettes may impair gut homeostasis primarily via modulation of host responses to microbes.

DISCUSSION

E-cigarettes trigger gut inflammation

The major discovery we report in this work is that chronic repetitive, but not acute, exposure to e-cigarette aerosols disrupts the gut epithelial barrier, increases the susceptibility of the gut lining to bacterial infections, and triggers gut inflammation (*Right*; Figure 6). We also show the components in the e-liquid as the major culprit (expanded upon later in "Discussion"). We established causality by using near physiologic *ex vivo* murine and human gut models (*Left*; Figure 6); the minimalistic nature of the polarized enteroid monolayer system and our ability to manipulate it in a physiologically relevant manner allowed us to pinpoint the target cell for e-cig-induced injury as the gut epithelial cell. It is possible that the barrier-disruptive injury is a direct consequence of the heat-decomposed chemical components in the e-cig vapor or is caused indirectly via secondary metabolites or the cytokines generated from EDMs. By using invasive *E. coli* in co-culture studies with EDMs, we also determine that handling of microbes by the gut epithelium was fundamentally impaired upon chronic and repetitive exposure to e-cig, resulting in higher infectivity and inflammation. These findings are in keeping with prior studies showing higher infectivity and inflammation in the epithelial lining of the oral mucosa (Pushalkar et al., 2020) and the lung (Crotty Alexander et al., 2018; Madison et al., 2019; Miyashita et al., 2018).

E-cigarettes broadly impact gut health

Our RNA-seq studies showed three major inter-related themes of altered transcriptional programs. The first are the pathways concerning cellular response to stress and stimuli comprising prominent inductions of genes that participate within the PPAR and AMPK signaling pathways. The second are the pathways concerning mucosal response to infection and inflammation, with prominent induction of genes that encode the anti-microbial peptide β-defensins and downregulation of multiple genes that modulate lysosomal biogenesis and *Tecpr1,* which is necessary and sufficient for autophagic clearance of microbes (Ogawa et al., 2011). The upregulation of stress response genes and the very specific pattern of upregulation of β-isoform of defensins are not unique to the gut; transcriptomic analyses on human bronchial epithelium have documented the same previously (Shen et al., 2016). The third and final theme is that of a balanced upregulation of genes that support pro- and anti-oncogenic pathways and processes, the most prominent of which were genes involved in cellular differentiation, i.e., multiple keratins. Because a sufficient amount of keratin is needed for efficient stress protection in the colonic epithelia and because keratins play an essential role of maintaining the epithelial barrier and its downregulation in intestinal tissue has been correlated with the progression of IBD (Asghar et al., 2015; Dong et al., 2017), our findings suggest that the three themes of altered gene expression may be inter-related consequences of epithelial stress response to chronic stimuli (simultaneous exposure to e-cig and microbes) and inflammation.

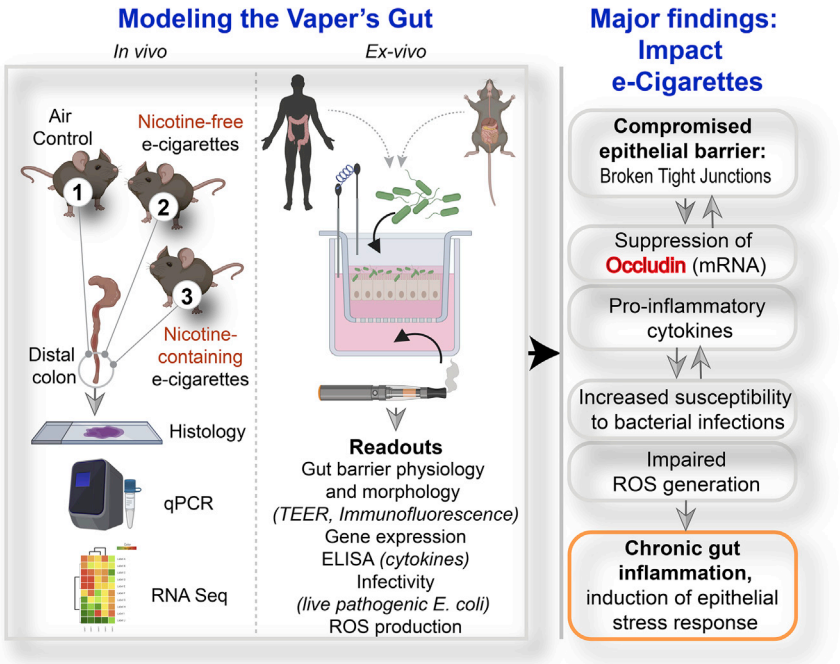

Figure 6. Summary of findings

Left: Schematic summarizes the various *in vivo* and *ex vivo* murine and human models used (top) and the readouts assessed (bottom) in this work to study the impact of vaping on the gut barrier. *Right*: The major findings and conclusions from this study showing how e-cig vapors can trigger distinct events (from top to bottom), such as epithelial barrier disruption, which is permissive to altered gene expression (lower occludin and higher cytokines), and heightened susceptibility for and response to bacterial infections, culminating in chronic inflammation and epithelial stress response. Potential feedforward loops that could set up a vicious loop of mucosal injury are indicated using bidirectional arrows.

E-liquid, not nicotine, is the culprit

Despite a vast array of literature pointing toward nicotine as a major source of ill-effects in people who smoke and vape, our RNA-seq studies using murine models of vaping unexpectedly but decisively revealed that it is the e-liquid component in e-cigarettes that induces broad and sweeping changes in gene expression in the gut. Virtually all changes in the distal colon were reversed by a concomitant co-administration of nicotine. These findings are in keeping with the barrier-tightening effect and anti-inflammatory effect of nicotine that have been demonstrated previously (Eliakim and Karmeli, 2003; Geng et al., 1996; Harries et al., 1982; Lashner et al., 1990; Madretsma et al., 1996; Prytz et al., 1989; Suenaert et al., 2000, 2003; Sykes et al., 2000; Van Dijk et al., 1995; Wang et al., 2012, 2016; Zhang and Petro, 1996). For example, exposure of epithelial monolayers to nicotine and its metabolites at concentrations corresponding to those reported in the blood of smokers significantly improves TJ integrity, and thus decreases epithelial gut permeability (Wang et al., 2012). Similarly, studies in humans (Prytz et al., 1989; Suenaert et al., 2000) have shown that nicotine does tighten the gut and that such effect may only be seen upon chronic, but not acute, exposures (Harries et al., 1982; Lashner et al., 1990; Suenaert et al., 2003). As for mechanism(s) behind such tightening, an upregulation of TJ markers (Wang et al., 2012, 2016), most prominently that of occludin, has been reported. Furthermore, nicotine has been generally found to serve as a protective factor for the development and progression of ulcerative colitis (Sykes et al., 2000), a condition that is characterized by leakiness of the gut barrier and chronic inflammation in the gut lining. When we tested the impact of e-cig on the gut barrier, we found that the nicotine-free vapors could disrupt the epithelial barriers in both murine (Figure S6) and human (Figures S7A–S7F) EDMs to a similar extent as vapors that contained nicotine. These findings are in keeping with other published work showing that it is the e-cig liquid alone (with PG/VG) that is sufficient for disrupting the proteome of bronchial epithelial cells (Ghosh et al., 2018) and suppressing bronchial epithelial cell ciliary motility (Clapp et al., 2019). The findings are also in keeping with the fact that nicotine is known to exert its anti-inflammatory action via nicotinic acetylcholinergic receptors (nAChRs) on monocytes (Madretsma et al., 1996; Sykes et al., 2000) and T cells (Geng et al., 1996; Zhang and Petro, 1996), presumably through the direct activation of the cholinergic anti-inflammatory pathway,

which involves inhibition of NF-κB signaling (Wang et al., 2003). That we see nicotine's anti-inflammatory action in mice (Figures 1 and 2) but do not see the same in EDMs (Figures S6 and S7) suggests that the observed anti-inflammatory action *in vivo* might be epithelium independent, but it is the e-cig base formulation containing PV/VG that is necessary and sufficient to destroy the gut barrier.

Translational relevance of findings

The gut is a complex environment; the gut mucosal barrier serves as the final frontier between the largest immune system in the body and trillions of microbes, diverse microbial products, food antigens, and toxins in the lumen. A compromised gut barrier allows microbes and antigens to leak through and encounter the host immune system, thereby generating inflammation and systemic endotoxemia. The compromised gut barrier is believed to be a major pathophysiologic component and a contributor to the initiation and/or progression of various chronic diseases, including, but not limited to, metabolic endotoxemia, type II diabetes, fatty liver disease, obesity, atherosclerosis, and IBDs. In documenting the harmful effects of e-cigarettes on the gut barrier, our study not just highlights the potential effects of e-cigarettes on the gastrointestinal tract but also provides insights into the potential long-term effects of e-cigarettes on health.

Limitations of the study

The safety of flavors and other additives (i.e., cannabinoids, THC) was not assessed here. In the absence of regulations over e-liquid contents and compositions and the plethora of flavors there is to test (thousands), scaling up to power such a study is not trivial. Another limitation is that the enteroid system is a minimalistic model and lacks critical components (e.g., immune and non-immune cells present under normal physiologic conditions) that are important for setting up a vicious cycle of inflammation in the gut and further damage of the epithelial lining. Thus, it is possible that the phenotypes observed in our EDM-based assays underestimate the full extent of injury and inflammation due to e-cigarettes. In fact, we believe that the missing immune cells in these assays could explain why there is an apparent discrepancy in the effects of e-cig and nicotine combinations observed *in vivo* versus those observed *in vitro* on EDMs. Finally, although we reconstitute the EDM model with live microbes (the single pathogenic strain of *AIEC-LF82*), the full impact of e-cigarettes in the setting of the polymicrobial gut luminal milieu was not estimated here. Ongoing work is investigating several of these outstanding aspects.

Resource availability

Lead contact

Further information and requests for resources and reagents should be directed to and will be fulfilled by the lead contact, Pradipta Ghosh (prghosh@health.ucsd.edu).

Materials availability

EDMs generated in this study will be made available on request, but we may require a payment and/or a completed Materials Transfer Agreement if there is potential for commercial application.

Data and code availability

This study has generated RNA-seq data of colon isolated from e-cigarette-treated mice. The RNA-seq datasets (metadata, RAW data, and processed data) generated in this work has been deposited at the NCBI GEO and can be queried using GSE161521.

METHODS

All methods can be found in the accompanying Transparent methods supplemental file.

SUPPLEMENTAL INFORMATION

Supplemental information can be found online at https://doi.org/10.1016/j.isci.2021.102035.

ACKNOWLEDGMENTS

This work was supported by awards from the Tobacco-Related Disease Research Program (TRDRP): 28IP-0024 (to P.G. and S.D.), 30IP-0965 and 26IP-0040 (to L.C.A.), the National Institutes of Health (NIH) grants DK107585 (to S.D.), AI141630 (to P.G.), R01HL147326 (to L.E.C.-A.) and R00-CA151673 (to D.S). S.D. was also supported by a DiaComp Pilot and Feasibility award (Augusta University). P.G., S.D., and D.S were

supported by NIH/National Center for Advancing Translational Sciences (NCATS) award UG3TR002968 and the Leonna M Helmsley Charitable Trust. S.-R.I. was supported by the NIH Diversity Supplement award. J.E. was supported by a Postdoctoral Fellowship from the American Cancer Society (PF-18-101-01-CSM). L.E.C.-A. was also supported by the American Heart Association (grant-in-aid 16BGIA27790079) and an ATS Foundation Award for Outstanding Early Career Investigators. This publication includes data generated at the UC San Diego IGM Genomics Center utilizing an Illumina NovaSeq 6000 that was purchased with funding from a National Institutes of Health SIG grant (#S10 OD026929). In addition, a P30 grant (NIH/NIDDK, P30DK120515) subsidized the RNA-seq and histology work showcased here. We are grateful to the HUMANOID CoRE for providing the media for the organoid culture.

AUTHOR CONTRIBUTIONS

A.S., J.L., A.G.F., A.M., T.K., I.M.S., and S.-R.I. designed and performed the experiments; R.F.P. and D.S. performed the RNA-seq analysis; J.E. performed and supervised the confocal microscopy experiments. A.S., J.L., A.G.F., P.G., and S.D. analyzed the data and generated the first draft of the manuscript; P.G. and S.D. wrote the manuscript. L.E.C.-A. provided expertise and access to the e-cigarette-infused media and e-cig treated murine colonic specimens; P.G., L.E.C.-A., and S.D. supervised the project.

DECLARATION OF INTERESTS

S.D. and P.G. have patents on methodology to prepare enteroid monolayers and functional assays related to the gut barrier. The authors have declared that no other conflict of interest exists.

Received: September 18, 2020
Revised: November 15, 2020
Accepted: December 31, 2020
Published: February 19, 2021

REFERENCES

Alasmari, F., Crotty Alexander, L.E., Hammad, A.M., Bojanowski, C.M., Moshensky, A., and Sari, Y. (2019). Effects of chronic inhalation of electronic cigarette vapor containing nicotine on neurotransmitters in the frontal cortex and striatum of C57BL/6 mice. Front Pharmacol. *10*, 885.

Alasmari, F., Crotty Alexander, L.E., Nelson, J.A., Schiefer, I.T., Breen, E., Drummond, C.A., and Sari, Y. (2017). Effects of chronic inhalation of electronic cigarettes containing nicotine on glial glutamate transporters and alpha-7 nicotinic acetylcholine receptor in female CD-1 mice. Prog.Neuropsychopharmacol. Biol. Psychiatry *77*, 1–8.

Allais, L., Kerckhof, F.M., Verschuere, S., Bracke, K.R., De Smet, R., Laukens, D., Van den Abbeele, P., De Vos, M., Boon, N., Brusselle, G.G., et al. (2016). Chronic cigarette smoke exposure induces microbial and inflammatory shifts and mucin changes in the murine gut. Environ.Microbiol. *18*, 1352–1363.

Asghar, M.N., Silvander, J.S., Helenius, T.O., Lahdeniemi, I.A., Alam, C., Fortelius, L.E., Holmsten, R.O., and Toivola, D.M. (2015). The amount of keratins matters for stress protection of the colonic epithelium. PLoS One *10*, e0127436.

Blount, B.C., Karwowski, M.P., Shields, P.G., Morel-Espinosa, M., Valentin-Blasini, L., Gardner, M., Braselton, M., Brosius, C.R., Caron, K.T., Chambers, D., et al. (2020). Vitamin E acetate in bronchoalveolar-lavage fluid associated with EVALI. N. Engl. J. Med. *382*, 697–705.

Boudeau, J., Glasser, A.L., Masseret, E., Joly, B., and Darfeuille-Michaud, A. (1999). Invasive ability of an Escherichia coli strain isolated from the ileal mucosa of a patient with Crohn's disease. Infect. Immun. *67*, 4499–4509.

Bozier, J., Chivers, E.K., Chapman, D.G., Larcombe, A.N., Bastian, N., Masso-Silva, J.A., Byun, M.K., McDonald, C.F., Alexander Crotty, L.E., and Ween, M.P. (2020). The evolving landscape of electronic cigarettes: a systematic review of recent evidence. Chest *157*, 1362–1390.

CDC, P H S, and United-States O o t S G. (2016). Office on Smoking and Health. E-Cigarette Use AmongYouth and Young Adults: AReport of the Surgeon General Atlanta (National Center for Chronic Disease Prevention and Health Promotion).

Clapp, P.W., Lavrich, K.S., van Heusden, C.A., Lazarowski, E.R., Carson, J.L., and Jaspers, I. (2019). Cinnamaldehyde in flavored e-cigarette liquids temporarily suppresses bronchial epithelial cell ciliary motility by dysregulation of mitochondrial function. Am. J. Physiol. Lung Cell Mol. Physiol. *316*, L470–L486.

Cox, S., Kosmider, L., McRobbie, H., Goniewicz, M., Kimber, C., Doig, M., and Dawkins, L. (2016). E-cigarette puffing patterns associated with high and low nicotine e-liquid strength: effects on toxicant and carcinogen exposure. BMC Public Health *16*, 999.

Crotty Alexander, L.E., Drummond, C.A., Hepokoski, M., Mathew, D., Moshensky, A., Willeford, A., Das, S., Singh, P., Yong, Z., Lee, J.H., et al. (2018). Chronic inhalation of e-cigarette vapor containing nicotine disrupts airway barrier function and induces systemic inflammation and multiorgan fibrosis in mice. Am. J. Physiol. Regul.Integr.Comp. Physiol. *314*, R834–R847.

Crotty Alexander, L.E., Ware, L.B., Calfee, C.S., Callahan, S.J., Eissenberg, T., Farver, C., Goniewicz, M.L., Jaspers, I., Kheradmand, F., King, T.E., Jr., et al. (2020). NIH workshop report: E-cigarette or vaping product use associated lung injury (EVALI): Developing a research agenda. Am. J. Respir. Crit. Care Med. *202*, 795–802.

Dawkins, L.E., Kimber, C.F., Doig, M., Feyerabend, C., and Corcoran, O. (2016). Self-titration by experienced e-cigarette users: blood nicotine delivery and subjective effects. Psychopharmacology (Berl) *233*, 2933–2941.

Dong, X., Liu, Z., Lan, D., Niu, J., Miao, J., Yang, G., Zhang, F., Sun, Y., Wang, K., and Miao, Y. (2017). Critical role of Keratin 1 in maintaining epithelial barrier and correlation of its down-regulation with the progression of inflammatory bowel disease. Gene *608*, 13–19.

Eliakim, R., and Karmeli, F. (2003). Divergent effects of nicotine administration on cytokine levels in rat small bowel mucosa, colonic mucosa, and blood. Isr. Med. Assoc. J. *5*, 178–180.

Etter, J.F., and Bullen, C. (2011). Electronic cigarette: users profile, utilization, satisfaction and perceived efficacy. Addiction *106*, 2017–2028.

Foulke-Abel, J., In, J., Kovbasnjuk, O., Zachos, N.C., Ettayebi, K., Blutt, S.E., Hyser, J.M., Zeng,

X.L., Crawford, S.E., Broughman, J.R., et al. (2014). Human enteroids as an ex-vivo model of host-pathogen interactions in the gastrointestinal tract. Exp. Biol. Med. (Maywood) *239*, 1124–1134.

Fricker, M., Goggins, B.J., Mateer, S., Jones, B., Kim, R.Y., Gellatly, S.L., Jarnicki, A.G., Powell, N., Oliver, B.G., Radford-Smith, G., et al. (2018). Chronic cigarette smoke exposure induces systemic hypoxia that drives intestinal dysfunction. JCI Insight *3*, e94040.

Furuse, M., Izumi, Y., Oda, Y., Higashi, T., and Iwamoto, N. (2014). Molecular organization of tricellular tight junctions. Tiss.Barr. *2*, e28960.

Geng, Y., Savage, S.M., Razani-Boroujerdi, S., and Sopori, M.L. (1996). Effects of nicotine on the immune response. II. Chronic nicotine treatment induces T cell anergy. J. Immunol. *156*, 2384–2390.

Ghosh, A., Coakley, R.C., Mascenik, T., Rowell, T.R., Davis, E.S., Rogers, K., Webster, M.J., Dang, H., Herring, L.E., Sassano, M.F., et al. (2018). Chronic E-cigarette exposure alters the human bronchial epithelial proteome. Am. J. Respir. Crit. Care Med. *198*, 67–76.

Ghosh, P., Swanson, L., Sayed, I.M., Mittal, Y., Lim, B.B., Ibeawuchi, S.R., Foretz, M., Viollet, B., Sahoo, D., and Das, S. (2020). The stress polarity signaling (SPS) pathway serves as a marker and a target in the leaky gut barrier: implications in aging and cancer. Life Sci. Alliance *3*, e201900481.

Gilbert, J.A., Quinn, R.A., Debelius, J., Xu, Z.Z., Morton, J., Garg, N., Jansson, J.K., Dorrestein, P.C., and Knight, R. (2016). Microbiome-wide association studies link dynamic microbial consortia to disease. Nature *535*, 94–103.

Harries, A.D., Baird, A., and Rhodes, J. (1982). Non-smoking: a feature of ulcerative colitis. Br. Med. J. *284*, 706.

Hua, M., Alfi, M., and Talbot, P. (2013). Health-related effects reported by electronic cigarette users in online forums. J. Med. Internet Res. *15*, e59.

Hwang, J.H., Lyes, M., Sladewski, K., Enany, S., McEachern, E., Mathew, D.P., Das, S., Moshensky, A., Bapat, S., Pride, D.T., et al. (2016). Electronic cigarette inhalation alters innate immunity and airway cytokines while increasing the virulence of colonizing bacteria. J. Mol. Med. *94*, 667–679.

Jones, R.M., Mercante, J.W., and Neish, A.S. (2012). Reactive oxygen production induced by the gut microbiota: pharmacotherapeutic implications. Curr. Med. Chem. *19*, 1519–1529.

Khlystov, A., and Samburova, V. (2016). Flavoring compounds dominate toxic aldehyde production during E-cigarette vaping. Environ. Sci. Technol. *50*, 13080–13085.

King, B.A., Jones, C.M., Baldwin, G.T., and Briss, P.A. (2020). The EVALI and youth vaping epidemics - implications for public health. N. Engl. J. Med. *382*, 689–691.

Kubota, K., Furuse, M., Sasaki, H., Sonoda, N., Fujita, K., Nagafuchi, A., and Tsukita, S. (1999). Ca(2+)-independent cell-adhesion activity of claudins, a family of integral membrane proteins localized at tight junctions. Curr. Biol. *9*, 1035–1038.

Lashner, B.A., Hanauer, S.B., and Silverstein, M.D. (1990). Testing nicotine gum for ulcerative colitis patients.Experience with single-patient trials. Dig. Dis. Sci. *35*, 827–832.

Lee, H.W., Park, S.H., Weng, M.W., Wang, H.T., Huang, W.C., Lepor, H., Wu, X.R., Chen, L.C., and Tang, M.S. (2018). E-cigarette smoke damages DNA and reduces repair activity in mouse lung, heart, and bladder as well as in human lung and bladder cells. Proc. Natl. Acad. Sci. U S A *115*, E1560–E1569.

Madison, M.C., Landers, C.T., Gu, B.H., Chang, C.Y., Tung, H.Y., You, R., Hong, M.J., Baghaei, N., Song, L.Z., Porter, P., et al. (2019). Electronic cigarettes disrupt lung lipid homeostasis and innate immunity independent of nicotine. J. Clin.Invest. *129*, 4290–4304.

Madretsma, G.S., Donze, G.J., van Dijk, A.P., Tak, C.J., Wilson, J.H., and Zijlstra, F.J. (1996). Nicotine inhibits the in vitro production of interleukin 2 and tumour necrosis factor-alpha by human mononuclear cells. Immunopharmacology *35*, 47–51.

Mahe, M.M., Aihara, E., Schumacher, M.A., Zavros, Y., Montrose, M.H., Helmrath, M.A., Sato, T., and Shroyer, N.F. (2013). Establishment of gastrointestinal epithelial organoids. Curr.Protoc. Mouse Biol. *3*, 217–240.

Margham, J., McAdam, K., Forster, M., Liu, C., Wright, C., Mariner, D., and Proctor, C. (2016). Chemical composition of aerosol from an E-cigarette: aquantitative comparison with cigarette smoke. Chem. Res. Toxicol. *29*, 1662–1678.

Miyashita, L., Suri, R., Dearing, E., Mudway, I., Dove, R.E., Neill, D.R., Van Zyl-Smit, R., Kadioglu, A., and Grigg, J. (2018). E-cigarette vapour enhances pneumococcal adherence to airway epithelial cells. Eur. Respir. J. *51*, 1701592.

Miyoshi, H., and Stappenbeck, T.S. (2013). In vitro expansion and genetic modification of gastrointestinal stem cells in spheroid culture. Nat. Protoc. *8*, 2471–2482.

Mravec, B., Tibensky, M., Horvathova, L., and Babal, P. (2020). E-cigarettes and cancer risk. Cancer Prev. Res. (Phila) *13*, 137–144.

Muthumalage, T., Prinz, M., Ansah, K.O., Gerloff, J., Sundar, I.K., and Rahman, I. (2017). Inflammatory and oxidative responses induced by exposure to commonly used e-cigarette flavoring chemicals and flavored e-liquids without nicotine. Front. Physiol. *8*, 1130.

Noel, G., Baetz, N.W., Staab, J.F., Donowitz, M., Kovbasnjuk, O., Pasetti, M.F., and Zachos, N.C. (2017). A primary human macrophage-enteroid co-culture model to investigate mucosal gut physiology and host-pathogen interactions. Sci. Rep. *7*, 45270.

Ogawa, M., Yoshikawa, Y., Kobayashi, T., Mimuro, H., Fukumatsu, M., Kiga, K., Piao, Z., Ashida, H., Yoshida, M., Kakuta, S., et al. (2011). A Tecpr1-dependent selective autophagy pathway targets bacterial pathogens. Cell Host Microbe *9*, 376–389.

Perez, M., and Crotty Alexander, L.E. (2020). Why is vaping going up in flames? Ann. Am. Thorac.Soc. *17*, 545–549.

Prytz, H., Benoni, C., and Tagesson, C. (1989). Does smoking tighten the gut? Scand. J. Gastroenterol. *24*, 1084–1088.

Pushalkar, S., Paul, B., Li, Q., Yang, J., Vasconcelos, R., Makwana, S., Gonzalez, J.M., Shah, S., Xie, C., Janal, M.N., et al. (2020). Electronic cigarette aerosol modulates the oral microbiome and increases risk of infection. iScience *23*, 100884.

Scott, A., Lugg, S.T., Aldridge, K., Lewis, K.E., Bowden, A., Mahida, R.Y., Grudzinska, F.S., Dosanjh, D., Parekh, D., Foronjy, R., et al. (2018). Pro-inflammatory effects of e-cigarette vapour condensate on human alveolar macrophages. Thorax *73*, 1161–1169.

Shen, Y., Wolkowicz, M.J., Kotova, T., Fan, L., and Timko, M.P. (2016). Transcriptome sequencing reveals e-cigarette vapor and mainstream-smoke from tobacco cigarettes activate different gene expression profiles in human bronchial epithelial cells. Sci. Rep. *6*, 23984.

Singh, K.P., Lawyer, G., Muthumalage, T., Maremanda, K.P., Khan, N.A., McDonough, S.R., Ye, D., McIntosh, S., and Rahman, I. (2019). Systemic biomarkers in electronic cigarette users: implications for noninvasive assessment of vaping-associated pulmonary injuries. ERJ Open Res. *5*, https://doi.org/10.1183/23120541.00182-2019.

Smith, T.T., Heckman, B.W., Wahlquist, A.E., Cummings, K.M., and Carpenter, M.J. (2020). The impact of E-liquid propylene glycol and vegetable glycerin ratio on ratings of subjective effects, reinforcement value, and use in current smokers. Nicotine Tob. Res. *22*, 791–797.

Song, M.A., Reisinger, S.A., Freudenheim, J.L., Brasky, T.M., Mathe, E.A., McElroy, J.P., Nickerson, Q.A., Weng, D.Y., Wewers, M.D., and Shields, P.G. (2020). Effects of electronic cigarette constituents on the human lung: a pilot clinical trial. Cancer Prev. Res. (Phila) *13*, 145–152.

Stewart, C.J., Auchtung, T.A., Ajami, N.J., Velasquez, K., Smith, D.P., De La Garza, R., 2nd, Salas, R., and Petrosino, J.F. (2018). Effects of tobacco smoke and electronic cigarette vapor exposure on the oral and gut microbiota in humans: a pilot study. PeerJ *6*, e4693.

Suenaert, P., Bulteel, V., Den Hond, E., Geypens, B., Monsuur, F., Luypaerts, A., Ghoos, Y., and Rutgeerts, P. (2003). In vivo influence of nicotine on human basal and NSAID-induced gut barrier function. Scand. J. Gastroenterol. *38*, 399–408.

Suenaert, P., Bulteel, V., Den Hond, E., Hiele, M., Peeters, M., Monsuur, F., Ghoos, Y., and Rutgeerts, P. (2000). The effects of smoking and indomethacin on small intestinal permeability. Aliment.Pharmacol.Ther. *14*, 819–822.

Sussan, T.E., Gajghate, S., Thimmulappa, R.K., Ma, J., Kim, J.H., Sudini, K., Consolini, N., Cormier, S.A., Lomnicki, S., Hasan, F., et al. (2015). Exposure to electronic cigarettes impairs pulmonary anti-bacterial and anti-viral defenses in a mouse model. PLoS One *10*, e0116861.

Sykes, A.P., Brampton, C., Klee, S., Chander, C.L., Whelan, C., and Parsons, M.E. (2000). An investigation into the effect and mechanisms of action of nicotine in inflammatory bowel disease. Inflamm. Res. *49*, 311–319.

Tang, M.S., Wu, X.R., Lee, H.W., Xia, Y., Deng, F.M., Moreira, A.L., Chen, L.C., Huang, W.C., and Lepor, H. (2019). Electronic-cigarette smoke induces lung adenocarcinoma and bladder urothelial hyperplasia in mice. Proc. Natl. Acad. Sci. U S A *116*, 21727–21731.

Van Dijk, J.P., Madretsma, G.S., Keuskamp, Z.J., and Zijlstra, F.J. (1995). Nicotine inhibits cytokine synthesis by mouse colonic mucosa. Eur. J. Pharmacol. *278*, R11–R12.

Wang, B., Wu, Z., Ji, Y., Sun, K., Dai, Z., and Wu, G. (2016). L-glutamine enhances tight junction integrity by activating CaMK kinase 2-AMP-activated protein kinase signaling in intestinal porcine epithelial cells. J. Nutr. *146*, 501–508.

Wang, H., Yu, M., Ochani, M., Amella, C.A., Tanovic, M., Susarla, S., Li, J.H., Wang, H., Yang, H., Ulloa, L., et al. (2003). Nicotinic acetylcholine receptor alpha7 subunit is an essential regulator of inflammation. Nature *421*, 384–388.

Wang, H., Zhao, J.X., Hu, N., Ren, J., Du, M., and Zhu, M.J. (2012). Side-stream smoking reduces intestinal inflammation and increases expression of tight junction proteins. World J. Gastroenterol. *18*, 2180–2187.

Wu, Q., Jiang, D., Minor, M., and Chu, H.W. (2014). Electronic cigarette liquid increases inflammation and virus infection in primary human airway epithelial cells. PLoS One *9*, e108342.

Yu, V., Rahimy, M., Korrapati, A., Xuan, Y., Zou, A.E., Krishnan, A.R., Tsui, T., Aguilera, J.A., Advani, S., Crotty Alexander, L.E., et al. (2016). Electronic cigarettes induce DNA strand breaks and cell death independently of nicotine in cell lines. Oral Oncol. *52*, 58–65.

Zhang, S., and Petro, T.M. (1996). The effect of nicotine on murine CD4 T cell responses. Int. J. Immunopharmacol *18*, 467–478.

iScience, Volume *24*

Supplemental Information

E-cigarettes compromise the gut barrier and trigger inflammation

Aditi Sharma, Jasper Lee, Ayden G. Fonseca, Alex Moshensky, Taha Kothari, Ibrahim M. Sayed, Stella-Rita Ibeawuchi, Rama F. Pranadinata, Jason Ear, Debashis Sahoo, Laura E. Crotty-Alexander, Pradipta Ghosh, and Soumita Das

Supplementary Online Information

MATERIALS AND METHODS

Key Resource Table

REAGENT or RESOURCE	SOURCE	IDENTIFIER
Biological Samples		
C57B/L6 mice	ENVIGO/HARLAN	
Adherent Invasive Escherichia coli strain LF82 (*AIEC*-LF82)	Arlette Darfeuille-Michaud, Inserm	(Chassaing and Darfeuille-Michaud, 2011) (Darfeuille-Michaud et al., 2004) Darfeuille-Michaud, A
Human tissue biopsies	HUMANOID CoRE VA hospital, San Diego	UCSD HRPP Project ID190105
Primers (Mouse/Human)	Forward primer (3'- 5')	Reverse primer (3'- 5')
Mouse 18S qPCR primers	GTAACCCGTTGAACCCCATT	CCATCCAATCGGTAGTAGCG
Mouse ZO-1 qPCR primers	GGGAGGGTCAAATGAAGACA	GGCATTCCTGCTGGTTACAT
Mouse IL-6 qPCR primers	CCCCAATTTCCAATGCTCTCC	CGCACTAGGTTTGCCGAGTA
Mouse IL-1b qPCR primers	GAAATGCCACCTTTTGACAGT	CTGGATGCTCTCATCAGGACA
Mouse TNF-alpha qPCR primers	CCACCACGCTCTTCTGTCTA	AGGGTCTGGGCCATAGAACT
Mouse IL-8 qPCR primers	CCTGCTCTGTCACCGATG	CAGGGCAAAGAACAGGTCAG
Mouse MCP-1 qPCR primers	AAGTGCAGAGAGCCAGACG	TCAGTGAGAGTTGGCTGGTG
Mouse Occludin qPCR primers	CCTCCAATGGCAAAGTGAAT	CTCCCCACCTGTCGTGTAGT
Mouse Claudin-1 qPCR primers	CCCCCATCAATGCCAGGTATG	AGAGGTTGTTTTCCGGGGAC
Mouse Claudin-2 qPCR primers	CCTTCGGGACTTCTACTCGC	TCACACATACCCAGTCAGGC
Human IL-8 qPCR primers	GAGCACTCCATATGGCACAAA	ATGGTTCCTTCCGGTGGT
Human IL-6 qPCR primers	CCAGAGCTGTGCAGATGAGT	CTGCAGCCACTGGTTCTGT
Human IL-1b qPCR primers	CCACAGACCTTCCAGGAGAATG	GTGCAGTTCAGTGATCGTACAGG
Human MCP-1 qPCR primers	AGTCTCTGCCGCCCTTCT	GTGACTGGGGCATTGATTG
Human ZO-1 qPCR primers	CGGTCCTCTGAGCCTGTAAG	GGATCTACATGCGACGACAA
Human Occludin qPCR primers	TCAGGGAATATCCACCTATCACTTCAG	CATCAGCAGCAGCCATGTACTCT TCAC
Software programs		
Prism	Graphpad	https://www.graphpad.com/scientific-software/prism/
Illustrator	Adobe	https://www.adobe.com/products/illustrator.html
Leica Application Suite X (LAS X)	Leica Microsystems	https://www.leica-microsystems.com/products/microscope-software/p/leica-las-x-ls/
Image J	FIJI	https://imagej.net/Welcome
AxioImager Z1 microscope	Carl Zeiss MicroImaging	
Chemicals and Reagents		
Direct-zol RNA Miniprep Kit	Zymo Research	R2052
Human IL-8/CXCL8 DuoSet ELISA	R&D systems	DY208
Human CCL2/MCP-1 DuoSet ELISA	R&D systems	DY279
Zinc Formalin Fixative	Fischer Scientific	23313096
DMEM with 10% FBS	Thermo Fisher Scientific	11995073
Fetal bovine serum	SIGMA-Aldrich	F2442-500ML
SB431542 (an inhibitor for TGF-β type I receptor	Bio-Techne Sales corp	1614/50
Y27632 (ROCK inhibitor)	Tocris	1254
Advanced DMEM/F12	Thermo Fisher Scientific	12634028

Trypsin	Thermo Fisher Scientific	15090046
Prolong Gold	Thermo Fisher Scientific	P36930
DNA/RNA Oxidative Damage ELISA Kit	Cayman Chemical, USA	501130
Collagenase type II	Invitrogen	17101015
70-µm cell strainer	Thermo Fisher Scientific	22-363-548
Matrigel	CORNING	354234
Gentamicin	Thermo Fisher Scientific	15750060
Transwell inserts	Thermo Fisher Scientific	07-200-154
qScript™ cDNA SuperMix	Quantabio	101414-108
Methanol	ACS	EM-MX0485-3
Triton X-100	SIGMA-Aldrich	X100-500ML
Trypan Blue	Thermo Fisher Scientific	15250061
HTS Transwell®-96 Permeable Support with 0.4 µm PET Membrane	Corning	7369
Antibodies		
Anti-Occludin mouse monoclonal antibody (1:500)	Invitrogen	331500
Anti-ZO-1 rabbit polyclonal antibody (1:500)	GeneTex	GTX108627
Alexa Fluor 594 conjugated goat anti-rabbit IgG (1:500)	Invitrogen	A11012
Alexa Fluor 488 conjugated goat anti-mouse IgG (1:500)	Invitrogen	A11001
DAPI (1:1000)	Invitrogen	D1306
Instruments		
Countess II Automated Cell Counter	Thermo Fisher Scientific	AMQAX1000
Epithelial Volt/Ohm (TEER) Meter	WPI	SKU EVOM2
Automated TEER Measurement System (REMS AutoSampler, Version 6.02)	WPI	SYS-REMS
Corning HTS Transwell-96 Electrode	WPI	REMS-96C
Leica Automated Inverted Microscope	Leica Microsystems	Leica DMI4000 B

All methods involving human and animal subjects were performed in accordance with the relevant guidelines and regulations of the University of California San Diego and the NIH research guidelines.

Murine E-Cigarette aerosol exposures: Six to eight-week-old male or female C57BL/6 (Envigo) were acclimatized to the SciReq whole body exposure inhalation system for 30 min a day for 3 days prior to beginning e-cigarette exposures. Mice were placed into individual slots in the whole-body exposure system and exposed for 4 sec every 20 sec for 1 h/day, 5 d/wk, for 1 wk or 12 wks. Mice received e-cigarette vapor produced from e-liquid containing 70/30 propylene glycol and glycerol with nicotine (Sigma) at a concentration of 6 mg/mL or without nicotine. At the end of the exposure period, mice were anesthetized with 10mg/kg and 100 mg/kg of xylazine and ketamine, respectively.

Preparation of E-cigarette vapor-infused media: E-liquid mixture of 70% propylene glycol and 30% glycerol and 6mg/mL nicotine (purchased from Sigma) without flavors or additives were used. E-cigarette atomizer and the rechargeable battery were obtained from Scireq. The atomizer contains a Kangertech Subtank Plus (7mL), with a 0.15 ohm coil. Fresh e-cig vapor-infused media was created by activating the battery via application of negative pressure by the InExpose system (SciReq), the e-liquid was heated and drawn through the internal atomizer and then into a 60 ml syringe containing 10 ml of wash media (DMEM/F12 with HEPES, 10% FBS). The wash media was exposed to 50mLs of e-cig vapor generated from the vaporization of the e-cig liquid, (with or without 6 mg/ml nicotine) followed by a 12-second shake; this is repeated 30 times.

Human subjects: Human ileum and colonic biopsies were collected from healthy subjects undergoing routine colonoscopy for colon cancer screening using the protocol approved by the Human Research Protection Program Institutional Review Board (Project ID# 190105). For all the deidentified human subjects, information including age, ethnicity, gender, previous history of the disease, and the medication was collected from the chart following the rules of HIPAA. Each human participant was recruited to the study following an approved human research protocol and signed a consent form approved by the Human Research Protection Program at the University of California, San Diego. Each donor agrees that their gastro-intestinal specimens will be used to generate an enteroid line at UC San Diego's HUMANOID^{TM} Center of Research Excellence (CoRE) for functional studies.

Isolation of enteroids from mouse and ileum and colonic specimens of healthy human: Intestinal crypts, comprised of crypt-base columnar (CBC) cells, were isolated from both colonic tissue of mice; and human colonic and ileal tissue specimens using the previously published paper (Ghosh et al., 2020; Sayed et al., 2020c). In brief, intestinal crypts were dissociated from tissues by digesting with collagenase type I (2 mg/mL solution containing gentamicin 50 ug/mL). The plate was incubated in a CO_2 incubator at 37°C, mixing every 10 minutes with vigorous pipetting in-between incubations, while monitoring the release of single epithelial units from tissue structures by light microscopy. To inactivate collagenase, wash media (DMEM/F12 with HEPES, 10% FBS) was added to cells, filtered through a 70 µM cell strainer, centrifuged at 200g for 5 min and then the supernatant was aspirated, leaving a cell pellet. The number of viable intestinal stem cells was determined by the Trypan Blue Exclusion method using Countess II Automated Cell Counter. Epithelial units were resuspended in matrigel and 15µl of cell-Matrigel suspension was added to the wells of a 24-well plate on ice and incubated upside-down in a 37°C CO_2 incubator for 10 min, which allowed for polymerization of the matrigel. After 10 min of incubation, 500µL of 50% Conditioned Media (CM, prepared from L-WRN cells with Wnt3a, R-spondin and Noggin, ATCC® CRL-3276™ (Miyoshi and Stappenbeck, 2013) containing 10 µM Y27632 and 10 µM SB431542 were added to the suspension. For the human colonic specimens, an in-house

proprietary cocktail was added to the above media. The medium was changed every 2 days and the enteroids were either expanded or frozen in liquid nitrogen for biobanking.

Preparation of Enteroid-derived monolayers (EDMs): EDMs were prepared by dissociating single cells from enteroids and plated either in 24-well or 96-well transwell with a 0.4 μm pore polyester membrane coated with diluted Matrigel (1:40) in 5% conditioned media as done before (Ghosh et al., 2020; Sayed et al., 2020c). The single-cell suspension was seeded at a density of approximately $2x10^5$ cells/well (in case of 24-well) or $8x10^4$ cells/well (in case of 96-well) and EDMs were differentiated for 2-3 days in 5% CM. The media was changed every 24 hours and monitored under a light microscope to evaluate the EDM generation and quality. As expected, the expression of EDMs showed a significant reduction of the stemness marker lgr5 in EDMs (Ghosh et al., 2020; Sato et al., 2009; Sayed et al., 2020c).

The treatment of enteroid-derived monolayers (EDMs) with e-cigarette vapor-infused media for functional assays: The polarized differentiated EDMs were treated with media that was infused with either nicotine-free e-cigarette or with 6 mg/mL nicotine-containing e-cigarettes by adding the vapor-infused media to the basolateral compartment of the transwells for the indicated times. The cells were either stained for confocal microscopy or used for measurement of transepithelial electrical resistance (TEER) or mRNA isolation; and for the collection of supernatants from apical and basolateral sides.

The measurement of Transepithelial electrical resistance (TEER): Two different methods were used for the measurement of TEER in low- (LTP) and high-throughput (HTP) modes.

Manual, LTP: In 24-well, TEER was measured at 0 h, 1 h, 4 h, 8 h, and 24 h, following exposure to e-cigarette vapor infused media using the STX2 electrodes with digital readout by EVOM2 (WPI).

Automated, HTP: The TEER of 96-well transwell plate with EDMs was measured using WPI automated TEER Measurement System. WPI REMS-96C recording electrode was used to record TEER, compatible with Corning 96-well plate format. REMS-96C recording electrode was sterilized in 70% Ethanol, followed by rinse in PBS and media. The REMS-96C apical electrode was calibrated to measure TEER approximately 1 mm above transwell membrane. Transwell-read time set to 12sec/well. Once set-up complete, plate removed from incubator and TEER measured directly afterward; the same read sequence was repeated every subsequent read to mitigate TEER artifacts due to temperature fluctuations. TEER recorded by REMS AutoSampler were saved as .txt files; raw TEER values (in Ωs), are converted to normalized TEER values by Raw TEER in ohms (Ω) x surface area of transwell in cm^2 = ohms. cm^2 (SA=0.143 cm^2 for 96-well and 0.33 cm^2 for 24-well).

Infection of EDMs with Adherent Invasive *E. coli (AIEC*-LF82*):* Adherent Invasive *Escherichia coli* strain LF82 (*AIEC*-LF82), isolated from the specimens of Crohn's disease patient, was obtained from Arlette Darfeuille-Michaud (Darfeuille-Michaud et al., 2004). For experimental use, a single colony was inoculated into LB broth and grown for 8 h under aerobic conditions and then under oxygen-limiting conditions overnight. 24h following treatment with e-cig vaped media, cells in the transwells were infected apically with a multiplicity of infection (moi) of 30 for 3 h. For gentamicin protection assay, bacteria were removed after 3h and treated with 200 μg/ml of gentamicin for 90 minutes, followed by serial dilution in 1x PBS and plating on LB agar plates. Colonies were counted the next day to measure colony forming unit per ml (cfu/ml)

RNA isolation and qRT-PCR: RNA was isolated from mouse colon tissues and EDMs followed by cDNA synthesis, as per manufacturer's instructions. Quantitative Real-Time PCR was conducted for target genes and normalized to housekeeping gene 18S rRNA. Fold change of treatment conditions was determined relative to the control condition. All primer sequences used in the study are provided in the key resource Table above.

RNA Seq and pathway enrichment analyses: RNASeq data was processed via kallisto (Bray et al., 2016) using the human genome build GRCh38 ensembl version 94 and corresponding genome annotation file to compute TPM (Transcripts Per Millions) (Li and Dewey, 2011; Pachter, 2011) values. We used log2(TPM+1) to compute the final log-reduced expression values. StepMiner (Sahoo et al., 2007) algorithm was used to compute a threshold for the high and low values for each gene. To generate the heatmap, a modified Z-score approach with StepMiner threshold (formula = (expr -SThr)/3*stddev) was used to further normalize the gene expression values. R version 3.2.3 (2015-12-10) was used to perform all statistical tests. We used python scipy.stats.ttest_ind package (version 0.19.0) with Welch's Two Sample t-test (unpaired, unequal variance (equal_var=False), and unequal sample size) parameters. For multiple hypothesis correction, *p* values were adjusted with statsmodels.stats.multitest.multipletests (fdr_bh: Benjamini/Hochberg principles). R statistical software (R version 3.6.1; 2019-07-05) was used to independently validate the results.

Over-representation (KEGG, GO, etc) analyses were carried out using the **g:GOSt** platform on p:Profiler (https://biit.cs.ut.ee/gprofiler/gost). The g:GOSt platform performs functional over-representation analysis (ORA) on input gene lists and identify statistically significantly enriched terms. The website curates data from Ensembl database and include pathways from KEGG, Reactome and WikiPathways; tissue specificity from Human Protein Atlas; protein complexes from CORUM and human disease phenotypes from Human Phenotype Ontology.

The RNA Seq dataset associated with this study can be accessed at NCBI GEO (GSE161521).

H& E staining: Colonic specimens were rinsed with phosphate-buffered saline (PBS) and fixed in zinc formalin for 24 h and embedded in paraffin. Paraffin sections (4 μm) were cut and de-waxed prior to immune-histochemical staining. Sections were stained with hematoxylin/eosin (H&E). Standard light microscopy was used to image tissue sections.

ELISA: Supernatant was collected from basolateral sides of EDMs and was examined for secreted cytokines, including IL-8 and MCP-1. These studies were done exactly as described previously (Sayed et al., 2020b; Sayed et al., 2020c) using biolegend kit as per manufacturer's protocol.

Measurement of oxidative DNA/RNA damage: The amount of oxidative DNA damage in untreated and e-cigarette treated EDMs before and after infection were quantified according to the manufacturer's instruction and previously published papers from others (Gao et al., 2019; Rodrigues et al., 2017) and from our own group (Sayed et al., 2020a; Sayed et al., 2020b). Briefly, supernatant from treated EDMs was used to detects oxidized guanine species: 8-hydroxy-2′-deoxaguanosine from DNA, and 8-hydroxyguanine from either DNA or RNA.

Immunofluorescence staining: Following the final TEER measurement, the media was removed from apical and basolateral compartments of all EDMs and gently washed 3 times with room temperature PBS, fixed with cold 100% methanol at 20°C for 20 min. Afterward, methanol was removed and washed with blocking buffer (0.1% Triton TX-100, 2 mg/mL BSA diluted in PBS) to permeabilize EDMs and to incubate with the following primary antibodies: ZO-1 (1:500) and Occludin (1:500). Primary antibodies were removed and washed with PBS 3 times for 5 min each time; after which the following secondary antibodies were added: Alexa Fluor 594 conjugated goat anti-rabbit IgG, Alexa Fluor 488 conjugated goat anti-mouse IgG and DAPI. Secondary antibodies were removed and washed with PBS 3 times for 5 min each time. To preserve fluorescence, monolayers were treaeded with Prolong Gold antifade reagent and stored at 4°C until imaged. Confocal Microscope with a 40x objective lens was used to image the stained EDMs. Z-stack images were acquired by successive 1 μm depth Z-slices of EDMs in the desired confocal channels of Leica TCS SP5 Confocal Microscope as done previously (Ghosh et al., 2020). Fields of view that were representative of a given transwell were determined by randomly imaging 3 different fields. Z-slices of a Z-stack were overlaid to create maximum intensity projection images; all images were processed using FIJI (Image J) software.

Statistical analysis

TEER, qPCR and ELISA results were expressed as the mean ± SEM and compared using a one-way ANOVA with Tukey's test or Mann-Whitney test. GraphPad Prism was used to analyze results and p-values < 0.05 was considered significant.

SUPPLEMENTARY TABLES

List of downregulated genes (n = 75)

B830042I05RIK	OTUD4	D430018E03RIK	GM20476	PKN2	AFTPH	SCYL3	EHF	1700028B04RIK	GM25219
MADCAM1	GM43213	GM17733	4732463B04RIK	ASXL2	IGHV 1-26	TRIM30A	HADHA	AW822252	SMG1
GM31774	ZBED6	CDK13	PTAR1	TRIM36	PRPF40A	SLC33A1	ACNAT1	ZFP871	TRPV3
GM12511	RPS10-PS1	HAO2	1700120E14RIK	RDH16F2	NAIP3	RANBP2	ZAN	ABCG2	TNPO1
GM26812	VAMP7	GM11945	MAP3K2	TECPR1	LY6C2	TMEM181B-PS	ETFDH	GM26711	SLC12A5
ZFP748	SLC12A3	GM44216	AL611930.1	ALG13	NUFIP2	GP2	SIRT3	PREPL	GM15693
CLDN12	RBM45	SH3GL2	MZB1	USP53	RCOR1	UNC13B	ATP6V0A2	TRIML1	GM9938
MOB1B	MYB	A1CF	EYA3	GAL3ST2c					

List of upregulated genes (n = 120)

CNIH2	SBSN	WFDC12	GM15519	TMPRSS11A	STFA1	CTCFLOS	TNNC2	ADIG	CYP1A1
LCE1D	SERPINB12	GM26751	PIN1	FAM178B	ENDOU	IL31RA	1700003F12RIK	CCDC27	DAPL1
MCPT4	GM32772	CNFN	KRT13	KRT10	DEFB14	CSTA1	MARC1	GM15551	GM94
GM12496	RETN	GP1bb	KRT6B	LGALS7	EAR2	BORCS5	Hp	GM10108	LCE1A2
LEP	CRCT1	GM48007	9330161L09RIK	AC164431.1	HOXD3OS1	LCE3F	GM11772	CALM4	PRKAB2
LCE3E	CCL8	APOC1	SLS36A2	LCE3B	LCE3A	DKKL1	KLK8	SPRR1A	LCE3C
IL1R2	TAGLN	SULT5A1	2300002M23RIK	LIPE	ARXES1	SLURP1	DEFB6	DEFB4	NNAT
SMOC1	EYA1	SCD1	RTL5	LOR	MT4	DISC1	NNMT	ARG1	GM47507
KRTAP20-2	ATP2A1	GAL3ST4	TMEM45A	TRIM29	TLCD2	FLG	SERPINB1C	S100A4	EMB
CAR3	SPRR4	SPRR3	LCE1A1	FABP4	FABP5	RNASE2B	GLB1L2	LCE1G	FCOR
STFA3	KRT1	A230028O05RIK	KRT5	KRT4	FAM25C	APOL6	KRT9	APOBR	RNF165
GM49339	ADIPOQ	PLIN1	ASPRV1	ILK	ADRB3	GM45716	SERPINB3a	GLRX5	BC100530

Supplementary Table S1 (related to Fig 2): Differentially regulated gene clusters in mice colon vaped with e-cigarette alone, versus e cigarette with nicotine.

SUPPLEMENTARY FIGURES AND LEGENDS

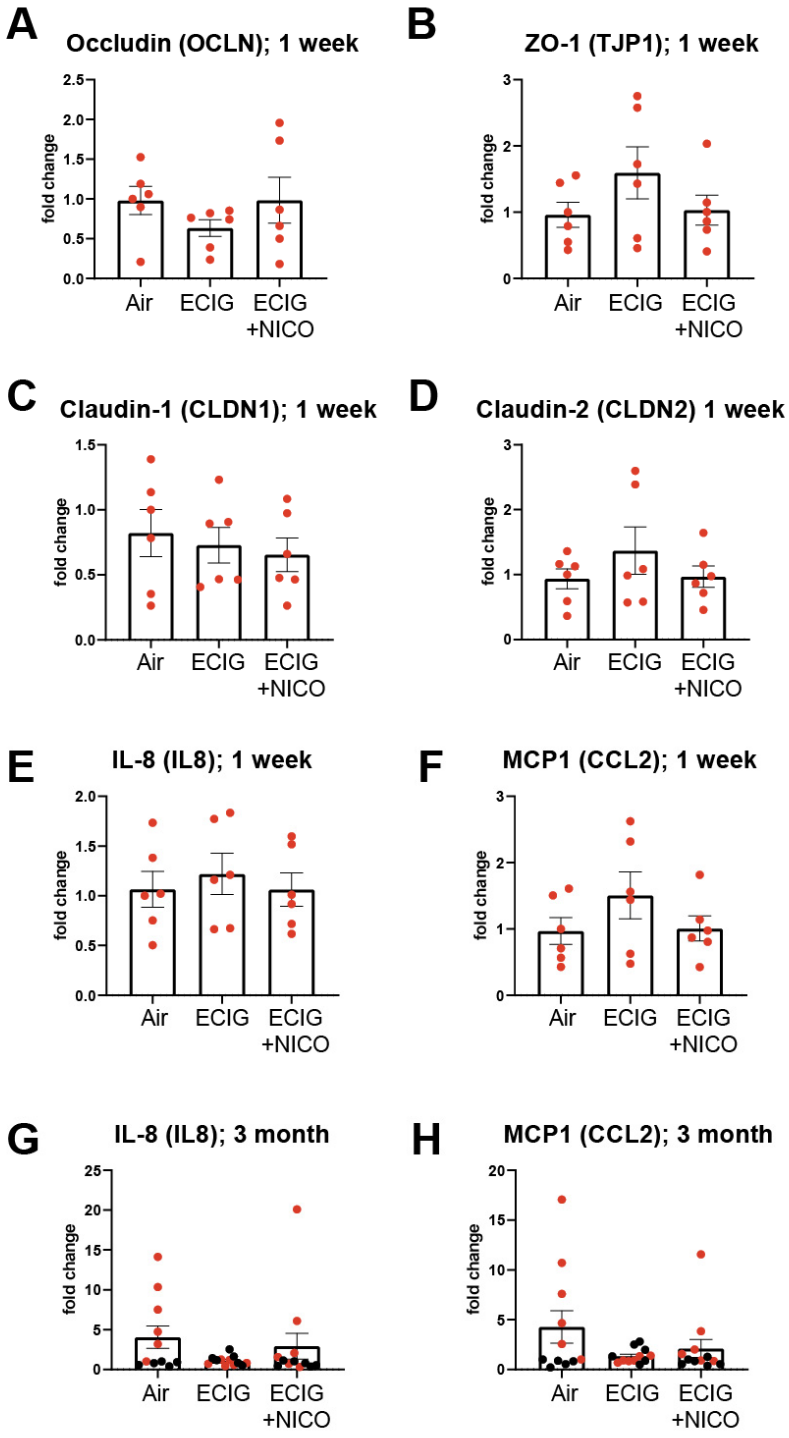

Figure S1. Gene expression changes after acute (1 week) or chronic (3 mo) of vaping (related to Fig 1). C57BL/6 mice were vaped using a special vaping chamber with MOD brand e-cigarette vapors (see **Fig 1A**), with (ECIG + NICO) and without (ECIG) 6 mg/ml nicotine for 1 week or 3 months by following specific regimen (details in methods), followed by isolation of the distal colon. The graphs represent the relative fold change in mRNA expression of tight junction markers (**A-D**) and pro-inflammatory cytokines (**E-H**) from 2-3 independent experiments with at least 4-5 mice/group of each experiment (Male mice = black data points; Female mice = red data points). Air = air control. Data represent as mean ± SEM. One-way ANOVA with Tukey's test was performed *$p < 0.05$, **$p < 0.01$ and ***$p < 0.001$.

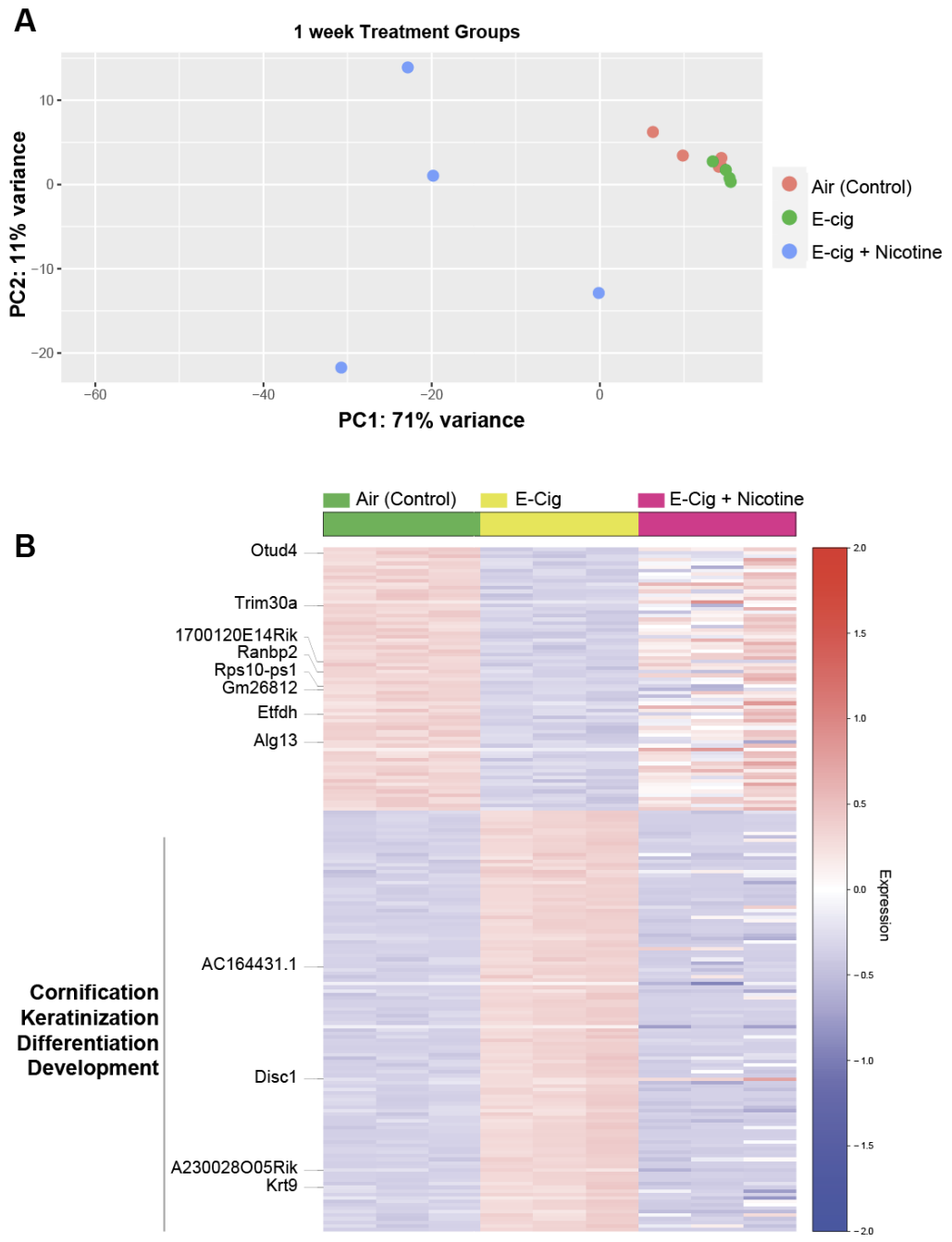

Figure S2. **Genes differentially expressed in mouse colon exposed to air or electronic cigarette (ECIG) vapors with and without nicotine (related to Fig 2)**. **A.** Principal component analysis of all 195 (75+120) genes by median absolute deviation. Colon exposed to e-cig vapors (green; n=4), e-cig with nicotine (purple, n =4), or Air (red; n=4). E-cig with nicotine samples differ from air controls and e-cig alone samples along with the first principal component, accounting for 71% of the variability in gene expression. **B.** Heatmap selectively highlighting those genes that are differentially expressed in air control (green) vs. e-cig alone (yellow) groups that are not rescued in the nicotine-containing e-cig group (magenta), as opposed to the large majority of them are indeed returned to levels in the control group (see **Fig 2B**). The upregulated genes support pathways (KEGG analysis) that concern differentiation, cornification and keratinization in the colon.

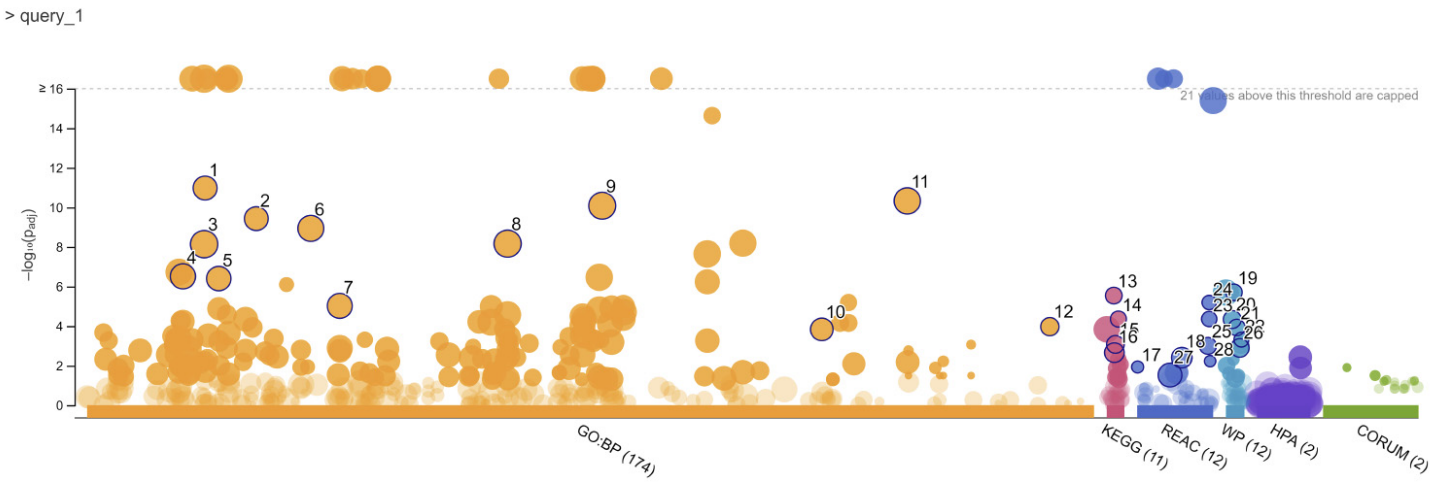

ID	Source	Term ID	Term Name	p_{adj} (query_1)
1	GO:BP	GO:0008219	cell death	1.060×10^{-11}
2	GO:BP	GO:0012501	programmed cell death	3.723×10^{-10}
3	GO:BP	GO:0008152	metabolic process	7.294×10^{-9}
4	GO:BP	GO:0006950	response to stress	3.077×10^{-7}
5	GO:BP	GO:0009605	response to external stimulus	3.978×10^{-7}
6	GO:BP	GO:0019538	protein metabolic process	1.161×10^{-9}
7	GO:BP	GO:0023051	regulation of signaling	9.560×10^{-6}
8	GO:BP	GO:0044238	primary metabolic process	6.869×10^{-9}
9	GO:BP	GO:0050896	response to stimulus	8.315×10^{-11}
10	GO:BP	GO:0098542	defense response to other organism	1.476×10^{-4}
11	GO:BP	GO:1901564	organonitrogen compound metabolic process	4.735×10^{-11}
12	GO:BP	GO:1990845	adaptive thermogenesis	1.076×10^{-4}
13	KEGG	KEGG:03320	PPAR signaling pathway	2.891×10^{-6}
14	KEGG	KEGG:04923	Regulation of lipolysis in adipocytes	4.425×10^{-5}
15	KEGG	KEGG:04152	AMPK signaling pathway	8.463×10^{-4}
16	KEGG	KEGG:04060	Cytokine-cytokine receptor interaction	2.201×10^{-3}
17	REAC	REAC:R-HSA-16...	AMPK inhibits chREBP transcriptional activation ac...	1.171×10^{-2}
18	REAC	REAC:R-HSA-67...	Neutrophil degranulation	3.959×10^{-3}
19	WP	WP:WP3942	PPAR signaling pathway	1.976×10^{-6}
20	WP	WP:WP236	Adipogenesis	4.642×10^{-5}
21	WP	WP:WP1403	AMP-activated Protein Kinase (AMPK) Signaling	1.179×10^{-4}
22	WP	WP:WP3965	Lipid Metabolism Pathway	4.876×10^{-4}
23	REAC	REAC:R-HSA-89...	Triglyceride metabolism	4.414×10^{-5}
24	REAC	REAC:R-HSA-16...	Triglyceride catabolism	6.438×10^{-6}
25	REAC	REAC:R-HSA-38...	Transcriptional regulation of white adipocyte differ...	1.004×10^{-3}
26	WP	WP:WP2877	Vitamin D Receptor Pathway	1.275×10^{-3}
27	REAC	REAC:R-HSA-16...	Immune System	3.004×10^{-2}
28	REAC	REAC:R-HSA-89...	VLDL clearance	5.944×10^{-3}

Figure S3. **Gene ontology (GO) analysis of differentially expressed genes the colons of mice exposed to e-cig compared to air controls (related to Fig 2).** Manhattan-like plots (top) represent the statistical enrichment (bottom) of pathways were generated using the list of differentially expressed genes and g:GOSt, a core of the g:Profiler that uses statistical enrichment analysis to interpret the functional relevance of gene signatures. The x-axis represents functional terms that are grouped and color-coded by data sources (e.g. GO biological process, orange; KEGG, magenta; Reactome, blue, etc). The y-axis shows the adjusted enrichment p-values in a negative log10 scale. The light circles represent insignificant terms (if available).

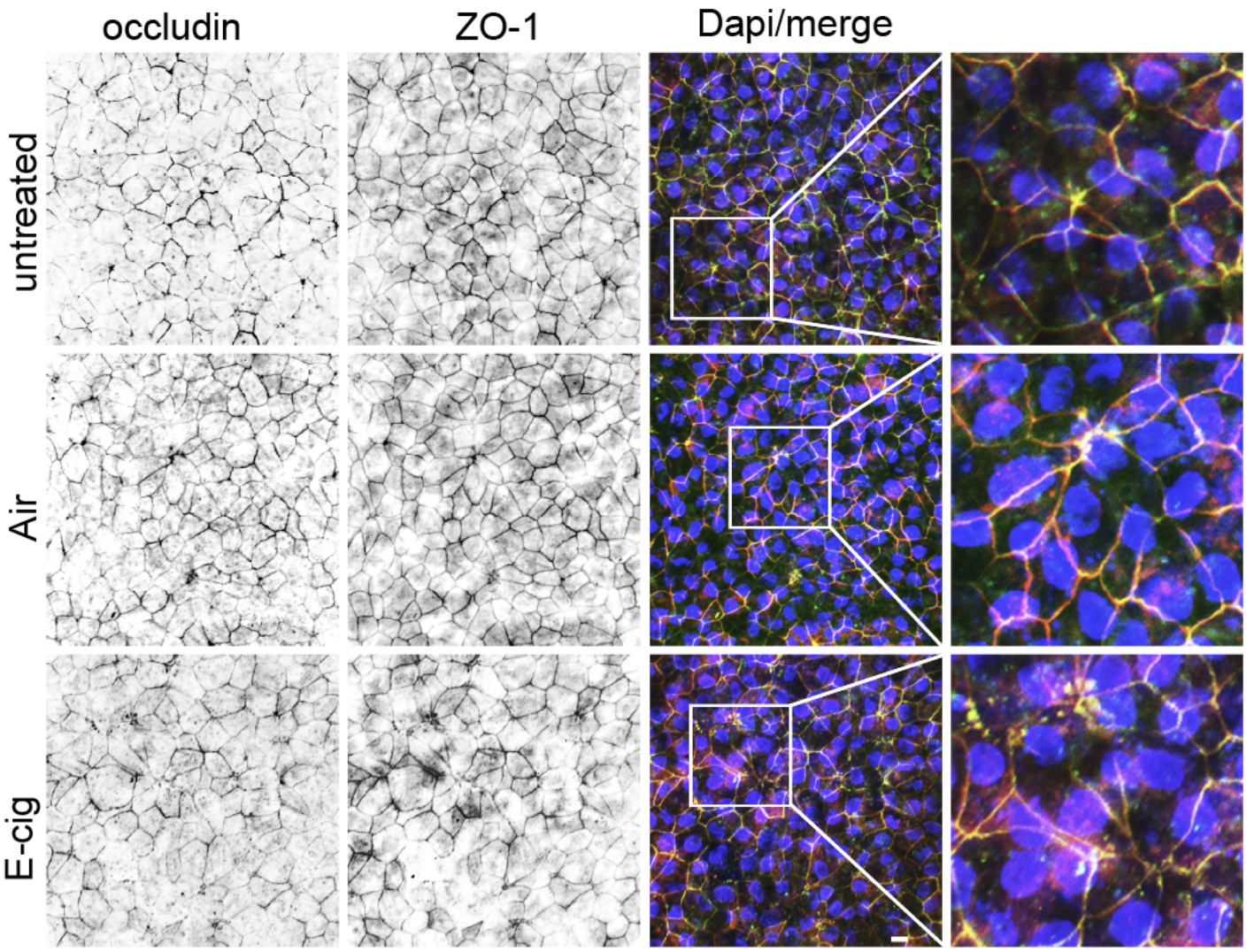

Figure S4. Confocal microscopic analysis of human EDMs after chronic exposure to e-cig vapor-infused media (related to Fig 3). Representative images show Occludin (a TJ marker; green), ZO-1(a TJ marker; red) and DAPI (blue, nuclei) in colonic EDMs either left untreated (top) for 24 h or exposed for the same duration to air (middle) or e-cig (bottom)-vapor-infused media. Scale bar = 10 μm. Cropped images on the right are presented in **Fig 3E**.

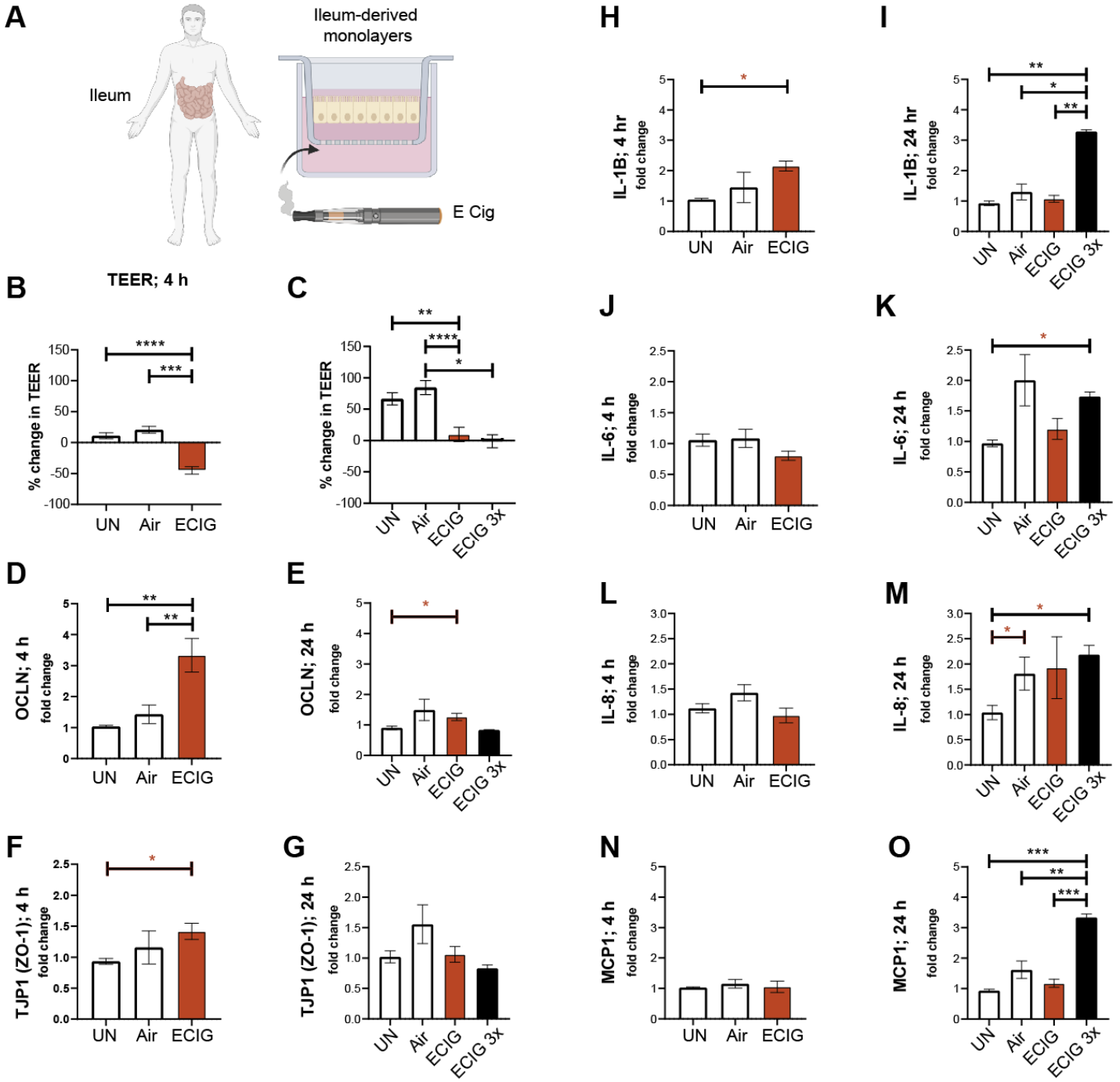

Figure S5. Nicotine-free e-cig disrupts the human ileal epithelial barrier, triggers inflammation (related to Fig 4). A. Schematic displays how enteroids isolated from ileal biopsies of healthy humans were differentiated into polarized enteroid-derived monolayers (EDMs) and exposed to e-cig vapor- infused media on the basolateral side. **B-C**. EDMs were either grown in normal media (UN) or treated with air-infused media (Air) or e-cig vapor-infused media (e-cig) and transepithelial electrical resistance (TEER) was measured over time. The graphs represented the percent change in Ω^*cm^2 from three independent experiments and displayed as mean ± SEM. Healthy ileal EDMs were maintained in media or treated with air-infused media or e-cigarette vapor- infused media. After acute exposure of 4 h and chronic exposure of 24 h, mRNA expression was measured after single or multiple exposures. The graphs represented the relative fold change compared to the EDM grown in normal media (UN) and mRNA expression of tight junction markers (**D-G**) and inflammatory cytokines (**H-O)** was measured from at least three independent experiments and displayed as mean ± SEM. One-way ANOVA with Tukey's test (black *) and Mann-Whitney (red *) test was performed *$p < 0.05$, **$p < 0.01$,***$p < 0.001$ and ****$p < 0.0001$.

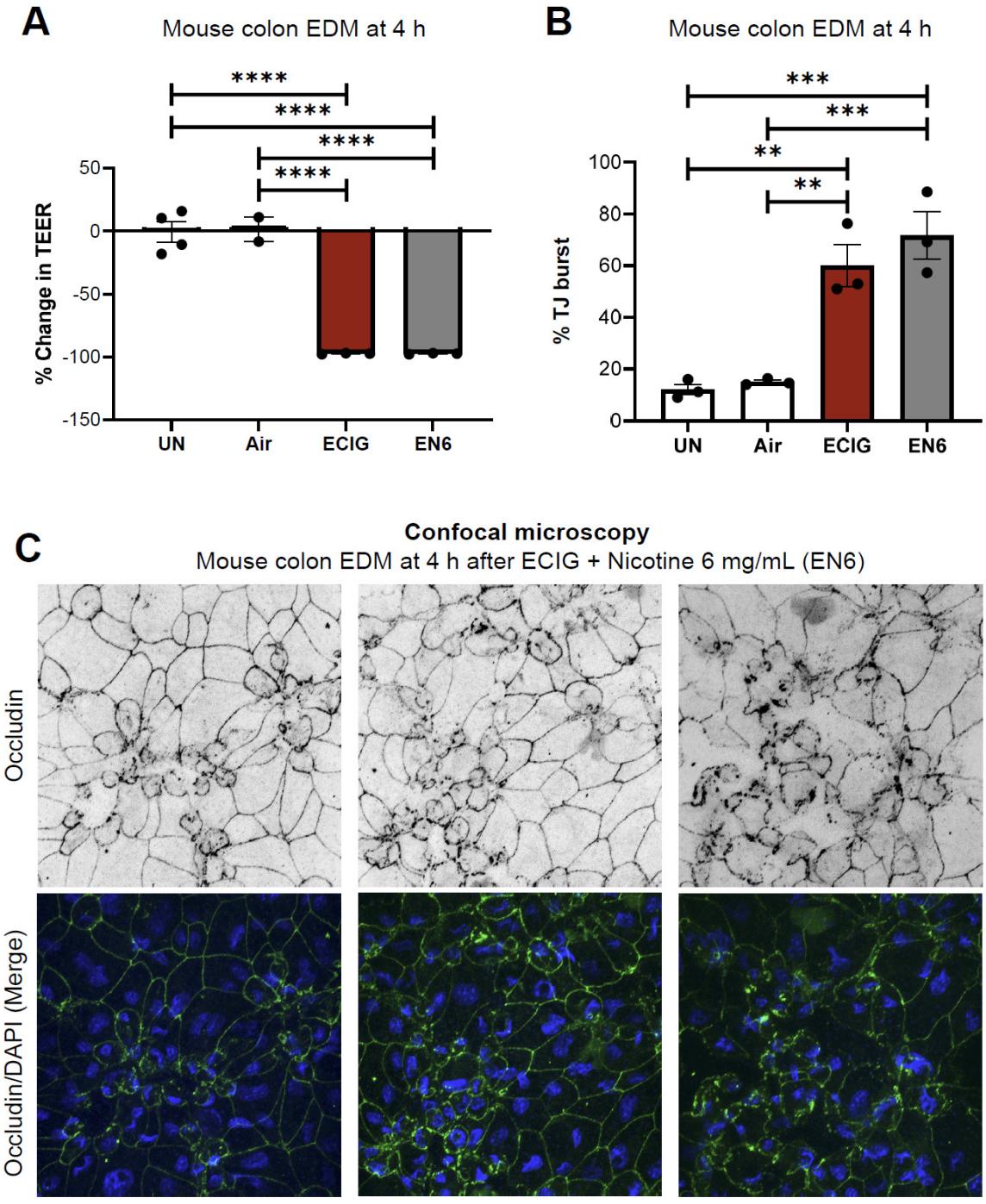

Figure S6. Media infused with vapors from nicotine-containing e-cig disrupt the integrity of the murine gut barrier to an extent similar to nicotine-free e-cig (related to Fig 4). A. Bar graphs display the percent change in TEER of murine EDMs after 4 h. EDMs were either grown in normal media (UN) or treated with air-infused media (Air) or e-cig vapor-infused media (ECIG) or e-cig with 6 mg/mL of nicotine vapor-infused media (EN6). Data is displayed as mean ± SEM (n = 3 independent experiments). **B-C.** EDMs were treated as indicated, fixed and stained for occludin (green) and DAPI (blue, nuclei) and analyzed by confocal microscopy. Bar graphs in **B** display the % increase in the tight junction (TJ) 'bursts' (indicative of disrupted TJs). Data is displayed as mean ± SEM (n = 3 fields/condition). Statistical significance was estimated using one-way ANOVA with Tukey's test; **$p < 0.01$, ,***$p < 0.001$ and ****$p < 0.0001$. Images in **C** display representative three different fields from EDMs after 4 h of treatment with e-cig containing 6 mg/mL of nicotine-infused media. Scale bar = 10 μm.

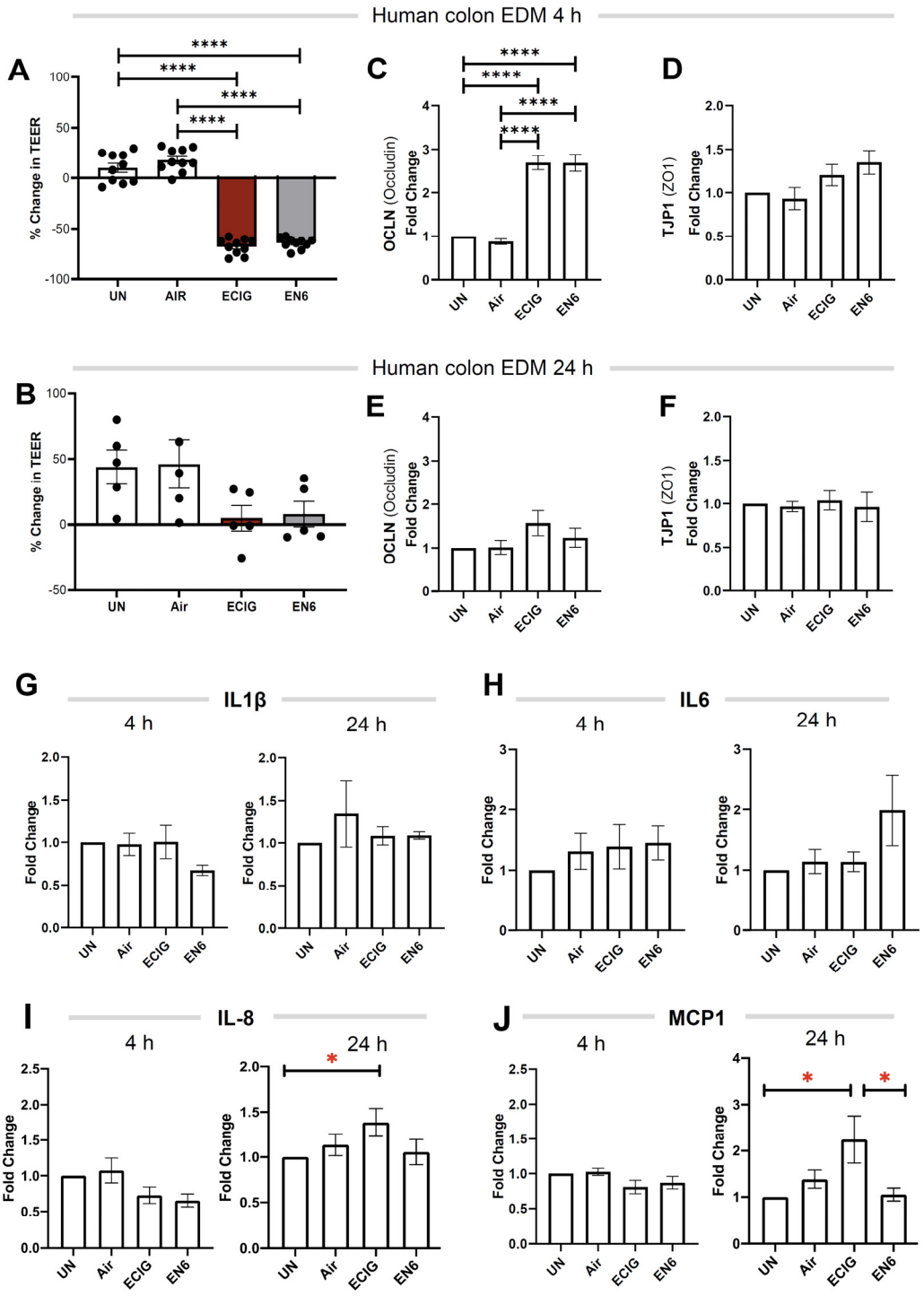

Figure S7. **Acute (4 h) and chronic (24 h) exposure to nicotine-free and nicotine-containing e-cigarettes decreases the TEER, alters the levels of markers of TJ and triggers inflammation to a similar extent (related to Fig 4).** (**A-B**) Bar graphs display the percent change in TEER of human colonic EDMs after 4 h (A) and 24 h (B) of the indicated treatments. EDMs were either grown in normal media (UN) or treated with air-infused media (Air) or e-cig vapor-infused media (ECIG) or e-cig with 6 mg/mL of nicotine vapor-infused media (EN6). Data is displayed as mean ± SEM (n = 5 independent experiments with 2 technical replicates for 4 h). (**C-F**) Bar graphs display the relative fold change in mRNA expression of TJ genes after 4 h (**C-D**) and 24 h (**E-F**) of the treatment. (**G-J**) Bar graphs display the relative fold change in mRNA expression of pro-inflammatory cytokines compared to the EDMs grown in normal media (UN) of genes from at least three independent experiments and displayed as mean ± SEM. One-way ANOVA with Tukey's test (black *) and Mann-Whitney (red *) test were performed. *$p < 0.05$, **$p < 0.01$ ***$p < 0.001$, ****$p < 0.0001$.

SUPPLEMENTARY REFERENCES

Bray, N.L., Pimentel, H., Melsted, P., and Pachter, L. (2016). Near-optimal probabilistic RNA-seq quantification. Nat Biotechnol *34*, 525-527.

Chassaing, B., and Darfeuille-Michaud, A. (2011). The commensal microbiota and enteropathogens in the pathogenesis of inflammatory bowel diseases. Gastroenterology *140*, 1720-1728.

Darfeuille-Michaud, A., Boudeau, J., Bulois, P., Neut, C., Glasser, A.L., Barnich, N., Bringer, M.A., Swidsinski, A., Beaugerie, L., and Colombel, J.F. (2004). High prevalence of adherent-invasive Escherichia coli associated with ileal mucosa in Crohn's disease. Gastroenterology *127*, 412-421.

Gao, X., Holleczek, B., Cuk, K., Zhang, Y., Anusruti, A., Xuan, Y., Xu, Y., Brenner, H., and Schottker, B. (2019). Investigation on potential associations of oxidatively generated DNA/RNA damage with lung, colorectal, breast, prostate and total cancer incidence. Sci Rep *9*, 7109.

Ghosh, P., Swanson, L., Sayed, I.M., Mittal, Y., Lim, B.B., Ibeawuchi, S.R., Foretz, M., Viollet, B., Sahoo, D., and Das, S. (2020). The stress polarity signaling (SPS) pathway serves as a marker and a target in the leaky gut barrier: implications in aging and cancer. Life Sci Alliance *3*.

Li, B., and Dewey, C.N. (2011). RSEM: accurate transcript quantification from RNA-Seq data with or without a reference genome. BMC Bioinformatics *12*, 323.

Miyoshi, H., and Stappenbeck, T.S. (2013). In vitro expansion and genetic modification of gastrointestinal stem cells in spheroid culture. Nat Protoc *8*, 2471-2482.

Pachter, L. (2011). Models for transcript quantification from RNA-Seq. In arXiv e-prints.

Rodrigues, D.G.B., de Moura Coelho, D., Sitta, A., Jacques, C.E.D., Hauschild, T., Manfredini, V., Bakkali, A., Struys, E.A., Jakobs, C., Wajner, M.*, et al.* (2017). Experimental evidence of oxidative stress in patients with l-2-hydroxyglutaric aciduria and that l-carnitine attenuates in vitro DNA damage caused by d-2-hydroxyglutaric and l-2-hydroxyglutaric acids. Toxicol In Vitro *42*, 47-53.

Sahoo, D., Dill, D.L., Tibshirani, R., and Plevritis, S.K. (2007). Extracting binary signals from microarray time-course data. Nucleic Acids Res *35*, 3705-3712.

Sato, T., Vries, R.G., Snippert, H.J., van de Wetering, M., Barker, N., Stange, D.E., van Es, J.H., Abo, A., Kujala, P., Peters, P.J.*, et al.* (2009). Single Lgr5 stem cells build crypt-villus structures in vitro without a mesenchymal niche. Nature *459*, 262-265.

Sayed, I.M., Chakraborty, A., Abd El Hafeez, A.A., A., S., Sahan, A.Z., WJM, H., Sahoo, D., Ghosh, P., Hazra, T.K., and Das, S. (2020a). The DNA Glycosylase NEIL2 Suppresses Fusobacterium-Infection-Induced Inflammation and DNA Damage in Colonic Epithelial Cells. Cells *9*.

Sayed, I.M., Sahan, A.Z., Venkova, T., Chakraborty, A., Mukhopadhyay, D., Bimczok, D., Beswick, E.J., Reyes, V.E., Pinchuk, I., Sahoo, D.*, et al.* (2020b). Helicobacter pylori infection downregulates the DNA glycosylase NEIL2, resulting in increased genome damage and inflammation in gastric epithelial cells. J Biol Chem *295*, 11082-11098.

Sayed, I.M., Suarez, K., Lim, E., Singh, S., Pereira, M., Ibeawuchi, S.R., Katkar, G., Dunkel, Y., Mittal, Y., Chattopadhyay, R.*, et al.* (2020c). Host engulfment pathway controls inflammation in inflammatory bowel disease. FEBS J *287*, 3967-3988.